Simulation of hydrodynamics and contaminant transport in artificial wetlands for partial gravity applications

Auteur : Nasir, Ahsan
Promoteur(s) : Richel, Aurore
Faculté : Gembloux Agro-Bio Tech (GxABT)
Diplôme : Master en bioingénieur : chimie et bioindustries, à finalité spécialisée
Année académique : 2024-2025
URI/URL : http://hdl.handle.net/2268.2/23325

European Master in Biological and Chemical Engineering for a Sustainable Bioeconomy

Master thesis report

submitted to obtain the degrees of

Master in Biology AgroSciences (BAS) of the University of Reims Champagne-Ardenne Master of Science in Engineering of Tallinn University of Technology

Master in Bioengineering: Chemistry and Bioindustries of the University of Liège

Title of the Master thesis

Simulation of hydrodynamics and contaminant transport in artificial wetlands for partial gravity applications

Presented by: **NASIR Ahsan**

Defended the: 25/06/2025

Supervised by

Patrick Grove, Louise Fleischer & Lucie Poulet

at

The Spring Institute for Forests on the Moon

&

University of Clermont-Auvergne (UCA)

from: 05/02/2025 to 31/07/2025

Bioceb supervisors:

Aurore Richel, ULiège

Niina Dulova, Taltech

Confidentiality: **No** Privacy expiration date:

This master thesis was developed under the supervision of The Spring Institute for Forests on the Moon at the Laboratoire de Génie des Procédés, Energétique et Biosystèmes (GePEB), Institut Pascal, University of Clermont-Auvergne (UCA) within the Erasmus Mundus Master program BIOCEB. The research was conducted under the supervision of Patrick Grove and daily supervision of Lucie Poulet and Louise Fleischer at the Génie des Procédés, Energétique et Biosystèmes (GePEB) at University of Clermont-Auvergne (UCA).

SUMMARY

Wastewater treatment and reuse are vital for sustainability on Earth, and now that long-duration space missions are being planned, developing compact, self-sufficient wastewater treatment systems is a pertinent challenge. This study explores the conceptual feasibility and simulation of a bioregenerative life support system (BLSS) based on a vertical flow constructed wetland (VFCW) for treating highly concentrated wastewater (up to 3000 mg/L COD), including solid waste, under partial gravity. Using the HYDRUS-2D model with the CW2D module, the study simulates variably unsaturated water flow and reactive solute transport through sand and lunar regolith simulant beds in a VFCW, under Earth and lunar gravity. Results show that the low permeability and high air-entry suction of lunar regolith in partial gravity significantly reduce infiltration rates and dissolved oxygen availability, which limits treatment efficiency. However, an optimized intermittent feeding strategy with extended resting periods (10-day downtime) enabled the lunar regolith system to achieve up to 95% COD removal. Comparative analysis revealed that sand outperforms lunar regolith simulant in continuous feeding scenarios but accumulates more inert sludge. The findings suggest that substrate selection, hydraulic properties, and feeding strategy are more critical than gravity alone in determining treatment success. The study provides recommendations for using lunar resources to build and operate a VFCW to treat the waste from a 4-astronaut base and offers insights for minimizing the footprint of CW installations on Earth.

Keywords: Vertical Flow Constructed Wetlands, Lunar Regolith Simulant, Partial Gravity Simulation

---

Résumé

Le traitement et la réutilisation des eaux usées sont essentiels à la durabilité sur Terre. Désormais, avec la planification de missions spatiales de longue durée, le développement de systèmes de traitement des eaux usées compacts et autonomes devient un défi crucial. Ce mémoire explore la faisabilité conceptuelle et la simulation d'un système de support de vie biogénératif (BLSS) basé sur un lit de macrophytes à écoulement vertical (VFCW) pour le traitement d'eaux usées très concentrées (jusqu'à 3000 mg/L de DCO), y compris les déchets solides, en gravité partielle. En utilisant le modèle HYDRUS-2D avec le module CW2D, l'étude simule l'écoulement de l'eau et le transport réactif des solutés à travers des lits de sable et de régolithe lunaire simulé (LMS-1), en gravité terrestre et lunaire. Les résultats montrent que la faible perméabilité et la forte pression d'entrée d'air du régolithe lunaire en gravité partielle réduisent significativement les taux d'infiltration et la disponibilité de l'oxygène dissous, ce qui limite l'efficacité du traitement. Cependant, une stratégie d'alimentation intermittente optimisée avec des périodes de repos prolongées (temps d'arrêt de 10 jours) a permis au système à base de régolithe lunaire d'atteindre jusqu'à 95 % d'élimination de la DCO. L'analyse comparative a révélé que le sable est plus performant que le LMS-1 dans des scénarios d'alimentation continue, mais qu'il accumule davantage de boues inertes. Les résultats suggèrent que le choix du substrat, les propriétés hydrauliques et la stratégie d'alimentation sont plus déterminants que la gravité seule pour assurer le succès du traitement. L'étude propose des recommandations pour l'utilisation de ressources lunaires dans la construction et l'exploitation d'un VFCW pour traiter les déchets de 4 astronautes, et offre des pistes pour réduire l'empreinte au sol des installations de CW sur Terre.

Mots clés: Lits de macrophytes à écoulement vertical, Régolithe lunaire simulé, Simulation en gravité partielle

---

LIST OF ABBREVIATIONS & SYMBOLS

Abbreviation	Full Form
VFCW	Vertical Flow Constructed Wetland
CW	Constructed Wetland
LRS	Lunar Regolith Simulant
LMS-1	Lunar Mare Simulant 1
LHS-1	Lunar Highland Simulant 1
PG	Partial Gravity
EG	Earth Gravity
COD	Chemical Oxygen Demand
rCOD	Readily Biodegradable COD
sCOD	Slowly Biodegradable COD
iCOD	Inert COD
DO	Dissolved Oxygen
BLSS	Bioregenerative Life Support System
ECLSS	Environmental Control and Life Support System
$\mathbf{K_{sat}}$	Saturated Hydraulic Conductivity
α	Inverse of Air Entry Suction Pressure
HYDRUS-2D	2D Water Flow and Solute Transport Simulation Software
CW2D	Constructed Wetland 2D Module (in HYDRUS)
EPA	Environmental Protection Agency (U.S.)
ISS	International Space Station
CFS	Continuous flow strategy
IFS	Intermittent flow strategy

GLOSSARY

Term	Definition
Air Entry Suction / Air Entry Value	The minimum suction (negative pressure) needed for air to begin entering the largest pores in a saturated medium. It indicates how easily a material can aerate after being wetted.
Chemical Oxygen Demand (COD)	A measure of the total amount of oxygen required to chemically oxidize organic and inorganic compounds in wastewater. It is used to estimate pollution levels.
Continuous Feeding Strategy (CFS)	A feeding approach in which wastewater is added to the wetland system continuously or in frequent, small doses. This improves flow rates but may limit oxygen availability due to saturation.
Constructed Wetland (CW)	A man-made system designed to simulate the water treatment functions of natural wetlands using vegetation, soil, and microbial processes.
Dissolved Oxygen (DO)	The amount of oxygen dissolved in water, essential for supporting aerobic microbial activity in biological treatment processes.
Feeding Strategy	The pattern or schedule of wastewater input to a constructed wetland. It affects saturation, oxygen levels, and treatment performance.
HYDRUS-2D	A modeling software used to simulate water flow, solute transport, and heat transfer in variably saturated porous media in two dimensions.
In-Situ Resource Utilization (ISRU)	The practice of using local materials (such as lunar regolith) for construction or system support, reducing the need for external supplies during space missions.
Intermittent Feeding Strategy (IFS)	A feeding method where wastewater is added in larger batches followed by rest periods. This allows the bed to re-aerate and promotes oxygen transfer for more efficient treatment.
Lunar Regolith Simulant (LRS)	A synthetic material developed to mimic the physical and chemical properties of lunar soil. Common types include LMS-1 (mare region) and LHS-1 (highland region).
Matric Potential	The pressure exerted by capillary and adsorptive forces that holds water within soil or porous media. It affects water availability and movement in unsaturated conditions.
Partial Gravity (PG)	A gravitational environment that is lower than Earth's gravity, such as on the Moon (1/6th of Earth's gravity). This influences water flow, oxygen diffusion, and treatment efficiency.
Reactive Transport	A modeling approach that accounts for both physical transport (e.g., water and solutes) and chemical/biological reactions occurring within the medium as it passes through the bed.
Saturated Hydraulic Conductivity (K_{sat})	A property that indicates how quickly water can move through a porous medium when fully saturated. Higher K_{sat} values mean faster water movement.
Van-Genuchten Model	A commonly used model to describe water retention and movement in unsaturated porous media. It uses parameters like α (related to air entry) and n (pore distribution).
Vertical Flow Constructed Wetland (VFCW)	A type of constructed wetland where wastewater is applied from the top and flows vertically through layers of substrate, allowing for filtration and biological treatment.
Water Content	The proportion of water present in a soil or substrate. It can be expressed as volumetric or gravimetric water content and affects the availability of water to plants and microbes.
Field Capacity of Soil	Field capacity is the amount of water soil retains after excess water has drained away due to gravity, allowing air to occupy pore spaces.

TABLE OF CONTENTS

Chapter 1: State-of-the-art

1.1 Context of the project

As efforts advance toward sustainable waste recovery systems, closing the loop in food and waste cycles remains a key challenge, particularly for long-duration space missions. A viable life support system in space must continuously recycle essential resources with minimal external input, given the limitations in material availability and manufacturing capacity. Current Environmental Control and Life Support Systems (ECLSS), such as those aboard the International Space Station (ISS), do not fully recycle wastewater and are inadequate for long-term missions[1].

A parallel constraint exists on Earth, where increasing urbanization and land scarcity demand compact, efficient wastewater treatment systems with low carbon and spatial footprints. For instance, the U.S. Environmental Protection Agency (EPA) recommends limiting the area footprint of wastewater treatment systems to 1 m^2 per person equivalent in urban settings[2].

Constructed wetlands (CWs) are engineered systems that replicate natural processes to purify wastewater. CWs have been explored as potential candidates for such systems, including early planetary base designs like Biosphere 2[3]. These systems utilize a combination of physical, chemical, and biological mechanisms to remove contaminants such as organic matter, nutrients (N and P) and suspended solids[4]. CWs offer several advantages, they are low-cost, energy-efficient, and require minimal technical supervision[5]. However, their large land requirements pose a significant limitation in urban and space-constrained environments. In this context, the present study aims to simulate a wastewater treatment for bioregenerative life support support system (BLSS) based on a vertical flow constructed wetland (VFCW) designed for lunar applications. The goal is to simulate the operation of this highly concentrated wastewater treatment process based under partial gravity conditions using in-situ resources from the lunar surface to support the feasibility of this project.

Chapter 1 presents the state-of-the-art and background relevant to the project. Chapter 2 outlines the mathematical modeling framework and parameter estimation methods used to develop the simulation approach. Chapter 3 details the simulation methodology and parameters. Chapter 4 presents and analyzes the results, providing insights into water dynamics and reactive transport in lunar regolith simulant under partial gravity. Chapter 5 discusses the key findings in the context of existing literature. Finally, Chapter 6 concludes the study and offers recommendations for design and operation and prototyping.

1.1.1 Current wastewater treatment methods for space applications

Current approaches to waste management in space, such as those used on the **International Space Station**, are largely focused on recovering water, with solid waste such as feces simply collected and discarded costing huge capital. Earth-based analogs for space missions also do not efficiently treat waste either. A 2005 survey of 71 Antarctic research stations found that only half had any wastewater treatment infrastructure, while the remaining discharged untreated sewage into crevasses permitted under the Protocol on Environmental Protection to the Antarctic Treaty [6]. Analog astronaut habitats are meant to simulate long-term human presence in space beyond Low Earth Orbit (LEO). Waste management at analog astronaut habitats is typically limited. For instance, the Mars Desert Research Station in Utah, United States, relies on septic tanks that are emptied post-mission[1]. Composting toilets, occasionally used for their simplicity, also often do not deliver meaningful nutrient recovery. Despite the implication of the term "composting," these systems mainly operate by dehydrating waste and venting off water vapor and gases, leaving behind minimal usable residue. Since compost is not circulated back into agricultural systems, these facilities remain dependent on regular deliveries of food, medicine, and other consumables. As we prepare for future exploration in space, the economic and logistical realities of resupply will necessitate more sustainable waste management and efficient recycling of all waste streams, including solid wastewater nutrients[1].

1.1.2 In-situ resource utilization (ISRU) for lunar exploration missions

In-Situ Resource Utilization (ISRU) is a critical approach for space exploration, involving the use of local resources to create products and services for robotic and human missions[7,8]. ISRU aims to reduce Earth launch mass, mission risks, and costs by producing essential consumables like propellants, life support materials, and manufacturing feedstock[7]. This technology can significantly enhance self-sufficiency, shielding, and infrastructure growth in space. ISRU systems must operate in various environments and gravities, considering diverse resource characteristics[8]. NASA has established an ISRU technology development program focusing on resources from the Moon such as lunar regolith excavation and oxygen production for future extended human missions to the Moon[9]. Therefore, depending upon the requirement, an early planetary base on the Moon could utilize lunar regolith excavated from the Moon surface to produce equipment and material for a bioregenerative life support system (BLSS). This presents an important opportunity for utilizing lunar regolith as a lunar resource for sustainable waste management.

1.2 Constructed wetlands (CW) for wastewater treatment

Marshes or wetlands are naturally occurring water reservoirs, where water is treated while feeding beneficial nutrients to the soil and developing plants on the surface. Marshes, fens, and bogs are diverse ecosystems with waterlogged soils and plant life that grow in these waterlogged conditions[10,11]. Wetlands

play an essential role in numerous ecological activities such as filtering water, blocking floods, and offering habitats for endangered species. Wetlands also play a major role in biogeochemistry and nutrient cycling regulation for silica, phosphorus, and nitrogen[12,13]. Wetlands have specific chemical transformation and transport properties that are often those of sinks for nutrients[13]. Wetlands can further act as a source of available nutrients during periods of low discharge, sustained by primary production, biomass storage, and microbial activity[14]. Wetland plant harvesting is a viable method for the removal of contaminant and retrieval of nutrients and energy.

1.2.1. Contaminant removal and types of CWs

The natural property of wetlands to treat and remove nutrients from water has been used to treat domestic and industrial wastewater, and such wetlands are called wastewater treatment wetlands or **constructed wetlands** (CW). CWs are man-made systems that strive to purify wastewater through natural processes [4]. These systems utilize physical, chemical, and biological mechanisms to remove impurities, including nitrogen, phosphorus, organic matter or chemical oxygen demand (COD), suspended solids, metals, and pathogens. The artificial wetlands are a low-energy, cost-effective solution when compared with conventional treatment methods[5]. Substrate, vegetation, and water are some of the natural components of CW that interact to create a natural treatment ecosystem [15]. CW substrate media options range from gravel to specialized materials like light-weight expanded clay aggregate (LECA) [16]. Various types of wastewaters, such as municipal, industrial, agricultural, and stormwater can be treated in a CW.

CWs are divided into two broad types: free water surface (FWS) and subsurface flow (SSF) wetlands. There are several types and orientations of CWs, in free water surface, subsurface flow (horizontal and vertical), and hybrid systems[17,18]. Despite their advantages, CWs require careful consideration of design parameters and may have higher land requirements compared to conventional systems [18,19]. This classification of wetlands is shown in Figure 1.1.

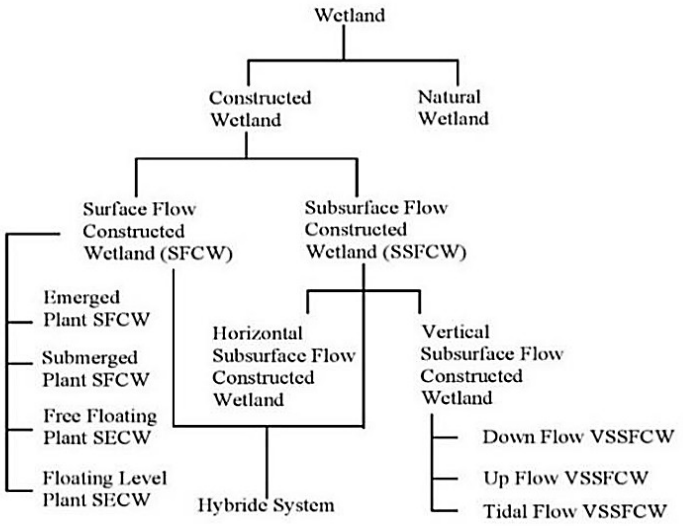

Figure 1.1: The figure shows the classification of various types of wetlands as shown by Swarnakar et al., 2022[19].

1.2.2 Vertical flow constructed wetlands (VFCWs)

Vertical subsurface flow constructed wetlands (VFCWs) are types of vertical geometry wetlands in which influent water infiltrates through the bed vertically, as shown in Figure 1.2. VFCWs have gained popularity due to their water conservation potential[20]. These systems demonstrate excellent performance in removing various pollutants, including COD, nitrogen, phosphorus, and coliforms. The design of VFCWs is optimizable by incorporating targeted pollutant removal levels. Oxygen transfer rate is a critical factor for sizing VFCWs, with newer designs allowing for more compact systems without resting periods[21]. Inflow rate, pollutant load, hydraulic retention time, and wetland design parameters affect nutrient removal[22]. Plant uptake also contributes to nutrient removal, although the harvesting timing is significant to achieve optimal efficiency[23].

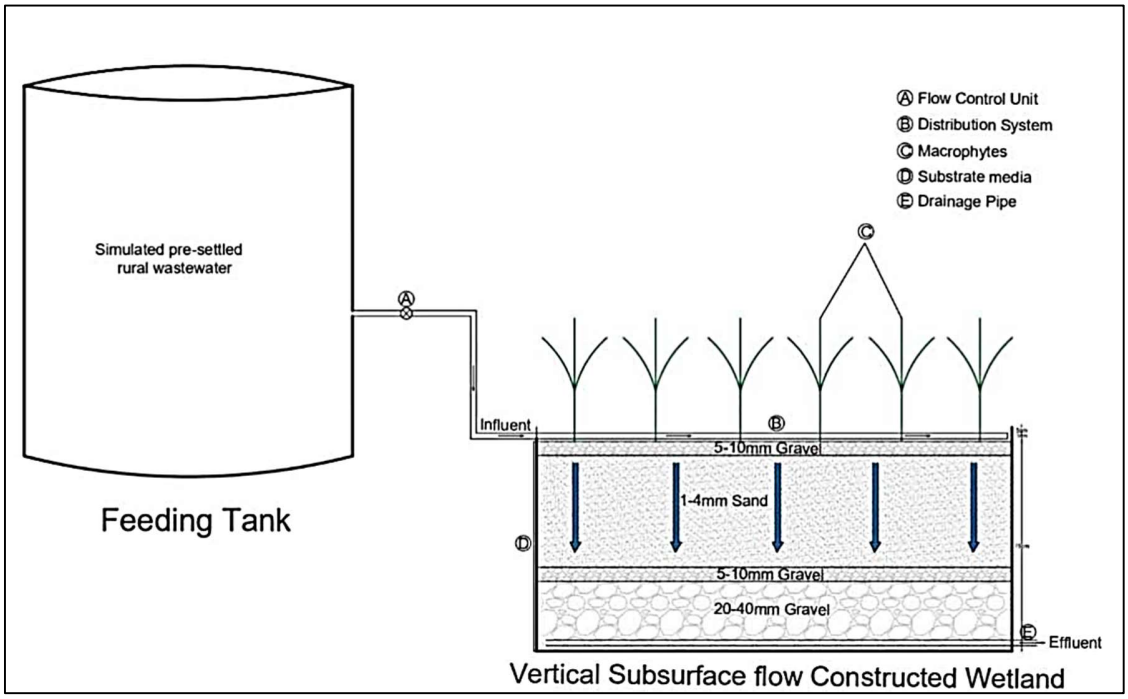

Figure 1.2: Figure shows the geometry of a typical VFCW with a feeding tank as shown by Shruthi et al., 2022[24].

Septic tanks combined with constructed wetlands offer an effective and low-cost solution for wastewater treatment. Studies have shown high removal rates for organic matter (87-89% COD, 88-97.5% BOD), nutrients (44-87% phosphorus, 63-86% nitrogen), and pathogens [25–28]. This kind of treated effluent often meets terrestrial irrigation water quality standards and can be safely used for hydroponic cultivation of vegetables[28]. These systems have demonstrated versatility and sustainability in various population dense geographical locations, including Egypt, India, Brazil, and China[25–28].

Microbial communities play a crucial role in contaminant removal, with aerobic degradation of organic matter, simultaneous nitrification, anaerobic ammonium oxidation (Anammox), and denitrification processes occurring in different zones of VFCWs. However, substrate clogging is a significant operational challenge in VFCWs, caused by the accumulation of suspended solids, microbial growth, and chemical precipitation[29]. Understanding hydrodynamic operation and interactions between various contaminant removal processes is essential for optimizing VFCW performance. Modeling approaches help elucidate these interactions and improve system design[30].

1.2.3 Operational strategies for VFCWs

VFCWs have various modifications in operation methods. The two main strategies are **continuous feeding strategy (CFS) and intermittent feeding strategy (IFS).** CFS is continuously addition of wastewater after a short time interval on to the bed without rest period (downtime). In IFS, wastewater is periodically applied to the surface and allowed to percolate downward through the filter media to a drainage layer at the base. This process involves multiple short dosing cycles per day (typically 4 to 12) followed by longer rest periods, during which the water gradually moves through the unsaturated substrate and the surface is able to dry. These intermittent loading cycles significantly improve oxygen exchange within the bed, promoting efficient aerobic biodegradation[31]. A new strategy is recirculating vertical flow constructed wetland (RVFCWs), is discussed in Sklarz et al., 2009[32]. Such a system is of interest because it allows the use of the same bed instead of having secondary treatment to reach the desired quality of effluent while requiring minimal area requirement. Even though recirculation presents a good alternative when spatial constraints are present, it adds extra machinery and parts to the system, which need to be maintained and run using additional resources.

Since VFCWs are complex systems in which water travels through porous media, the mechanisms of water movement are influenced by various factors. In unsaturated porous solids, water movement occurs under the influence of gravity, moisture, and temperature gradients, involving both liquid and vapor phases[33]. Capillary rise in porous media exhibits "jump" behavior at pore necks, with the wetting front appearing flat and saturated in initially dry conditions but irregular and unsaturated in initially wet conditions. Clogging primarily occurs in the upper layers and is caused by inorganic and organic suspended solids, biomembrane growth, and water adsorption[34]. This process affects hydraulic conductivity (the ability of water infiltration through the bed over time) and internal flow patterns over time[35].

1.2.4 Beds and substrates used in CWs and their contaminant removal mechanism

Various materials have been used as CW substrates, usually minerals, and the research for using various materials as CW substrates has been increasing over the years[36]. Depending on the nature of the substrate, it can remove particles and contaminants by making them stick by an adsorption mechanism shown in Figure 1.3 below. As the contaminant passes through the substrate's fluid-solid film and diffuses into the substrate and performs desorption of molecules [36]. The mathematical equation for this process is discussed in the next chapter. Substrate selection therefore influences treatment performance, with hydraulic conductivity and clogging capacity influencing performance. Gravel substrates are more conductive than sand-and-gravel mixtures, which are prone to clogging[37]. Substrate optimization through combination or alteration is recommended to enhance treatment performance. The substrate selection must

be designed to meet influent water quality and pollutant removal objectives, since no one substrate provides optimal treatment for all contaminants[36]. The diversity of substrates used for CW allows for possible speculation about using lunar regolith as a substrate in CWs. This possibility can allow for the use of this substrate instead of transporting soil or substrate from the Earth to serve as bedding for the system.

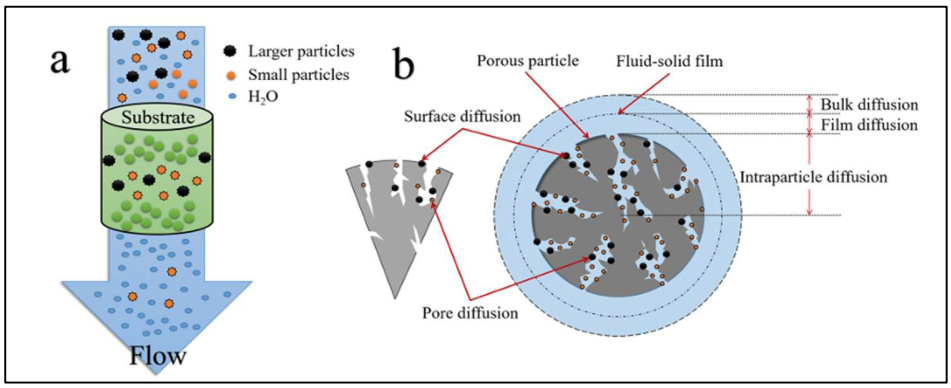

Figure 1.3: Figure shows the contaminant removal with the substrate (a) and adsorption mechanism as adapted from Yang et al., 2022.

1.2.5 Potential of lunar regolith as a substrate for wetland bed and lunar regolith simulants

Lunar regolith is a layer of loose, fragmented material covering the solid bedrock on the Moon's surface formed by continuous meteorite and micrometeorite impacts on the lunar surface. Its dust resembles that of sand but differs in characteristics from earth soil. It doesn't contain any organic matter or microorganisms or moisture. However, it has been speculated that the average ice content on the lunar poles is estimated to be 1.5 ± 0.8% by mass[38]. The particle size distribution of the lunar soil changes with the depth of excavation and is mostly consistent to a depth of several meters as shown in the Table A1 (Annex)[39].

Although lunar regolith is devoid of organic matter, nitrogen and other nutrients that are necessary for the growth of plants and a healthy microbiota, it contains one of the constituents in terrestrial soil i.e, mineral matter, and some amounts of dinitrogen (N_2) and oxygen gas (O_2). For lunar regolith to be used like terrestrial soils, all or some of the major components like organic matter is needed to be added into the regolith[40]. The diverse microbial communities in terrestrial soil maintain the soil's function and nutrient cycling process; these microbial communities, therefore, can be introduced into the soil for its maintenance and nutrient function. Heterotrophic microorganisms present in wetlands require organic matter for their survival. It has been suggested that terrestrial soil or deep groundwater with a stable microbial community can serve as an inoculum for the lunar regolith[40].

Lunar regolith differs in mechanical and chemical properties depending upon the location on the Moon and depth it is excavated from as shown in Figure A1 and Table A1 (Annex) respectively. To approximate the chemical, mechanical, engineering, mineralogical, or particle-size distribution properties of lunar regolith, scientists synthesize terrestrial materials called **lunar regolith simulants**. Lunar regolith simulants are crucial for testing equipment, evaluating health risks, and developing in ISRU for lunar exploration[41]. These simulants aim to replicate specific characteristics of lunar regolith, such as bulk chemistry, particle size, and distribution. However, terrestrial simulants differ from actual lunar regolith in elemental composition due to the Moon's unique environment[42]. While simulants have been invaluable for lunar mission preparations since the Apollo era, they are not perfect replicas of lunar regolith, and their use in terrestrial environments can affect experimental and simulation results[43]. The two important lunar regolith simulants in the context of this study are Lunar Mare Simulant (LMS-1) and Lunar Highland Simulant (LHS-1) and which have been shown to provide a good estimate of lunar regolith geomechanical properties {Citation}.

1.3 Potential effects of partial gravity and lunar conditions on VFCWs

An early planetary base on the Moon experiences reduced or partial gravity, which is $1/6^{th}$ of terrestrial gravity, i.e., 1.62 m/s^2. This is called "**partial gravity**" and can have a potentially overlooked effect on various processes, like hydrodynamics or water dynamics, that are important in a wetland system and might change the behavior of an ecosystem by changing common processes such transport through a porous bed. It is important to study the vertical gravity flow of water through the VFCWs in partial gravity. The hydrodynamics will determine how long it takes for the wetland to treat a certain amount of wastewater and the proper functioning of its wastewater treatment process. Water movement in porous media under reduced gravity conditions, such as on the Moon, involves complex mechanisms. For instance, in microgravity, conventional capillary flow does not fully explain water distribution, with evidence suggesting narrower pore size distributions and inactive large pores[44]. However, recent studies found no significant differences in infiltration rates between low gravity and Earth gravity (1G) conditions for fine uniform porous media[45]. Reduced gravity, such as partial gravity on the Moon's surface, can lead to unstable fluid displacement patterns and enhanced phase entrapment, potentially modifying macroscopic transport properties[44].

Microbial activity in extraterrestrial spaces is expected to differ significantly from Earth due to harsher conditions, including extreme temperatures, high radiation, and low pressure [46]. These factors have been causing rapid inactivation of microbes on external spacecraft surfaces, with a predicted -231 log reduction in viable bioburden per lunation at the equator[46]. However, internal spacecraft and base areas may harbor microbes longer[46]. Simulated lunar gravity studies suggest increased bacterial growth and higher antibiotic resistance for some strains compared to Earth conditions[47]. The lunar surface also exhibits unique radioactivity due to radon and thoron diffusion, estimated at approximately 1 microcurie per square meter[48].

These factors collectively contribute to a distinct microbial environment on the Moon compared to Earth, impacting potential lunar exploration efforts and contamination risks. While the synergistic effects on the activity of microorganisms of a VFCWs on the Moon cannot be simulated, insights can be provided by using terrestrial microbial models and empirical data to simulate the hydrodynamics and contaminant removal processes.

1.4 Objectives

Although ISRU has not been demonstrated in actual missions, it is crucial to evaluate concepts and technologies under relevant conditions and through simulation[7]. In this study, '*The Marshian*' concept (from the word 'Marsh') of a VFCW for wastewater treatment including solid waste from a lunar base[1]. Evaluation of feasibility of such a VFCW cannot be done without proper evidence for its operation in partial gravity conditions. Since experimental techniques lack the ability to simulate such a system in partial gravity, the systems need to be simulated based on a mathematical model by adapting terrestrial models adjusted to accommodate the effect of partial gravity. Therefore the aims of this study is to provide a simulation of the VFCW to meet the following objectives:

- To simulate the feasibility of treatment of high strength macerated wastewater with solid waste from a lunar base using a minimal area footprint and achieving 75% total COD removal (threshold limit)
- To simulate the VFCW's performance under partial gravity conditions (1/6th Earth gravity), for operation on the Moon with minimal machinery and human intervention
- To gain insights into water dynamics and biokinetics within the VFCW when using lunar regolith simulant as the substrate under partial gravity conditions and identify key functioning parameters
- To propose design and operation recommendations for prototype development and validating the feasibility using simulation results for a 4-person astronaut base

Figure 1.4 explains how the flow of the research and simulation efforts to achieve the objectives.

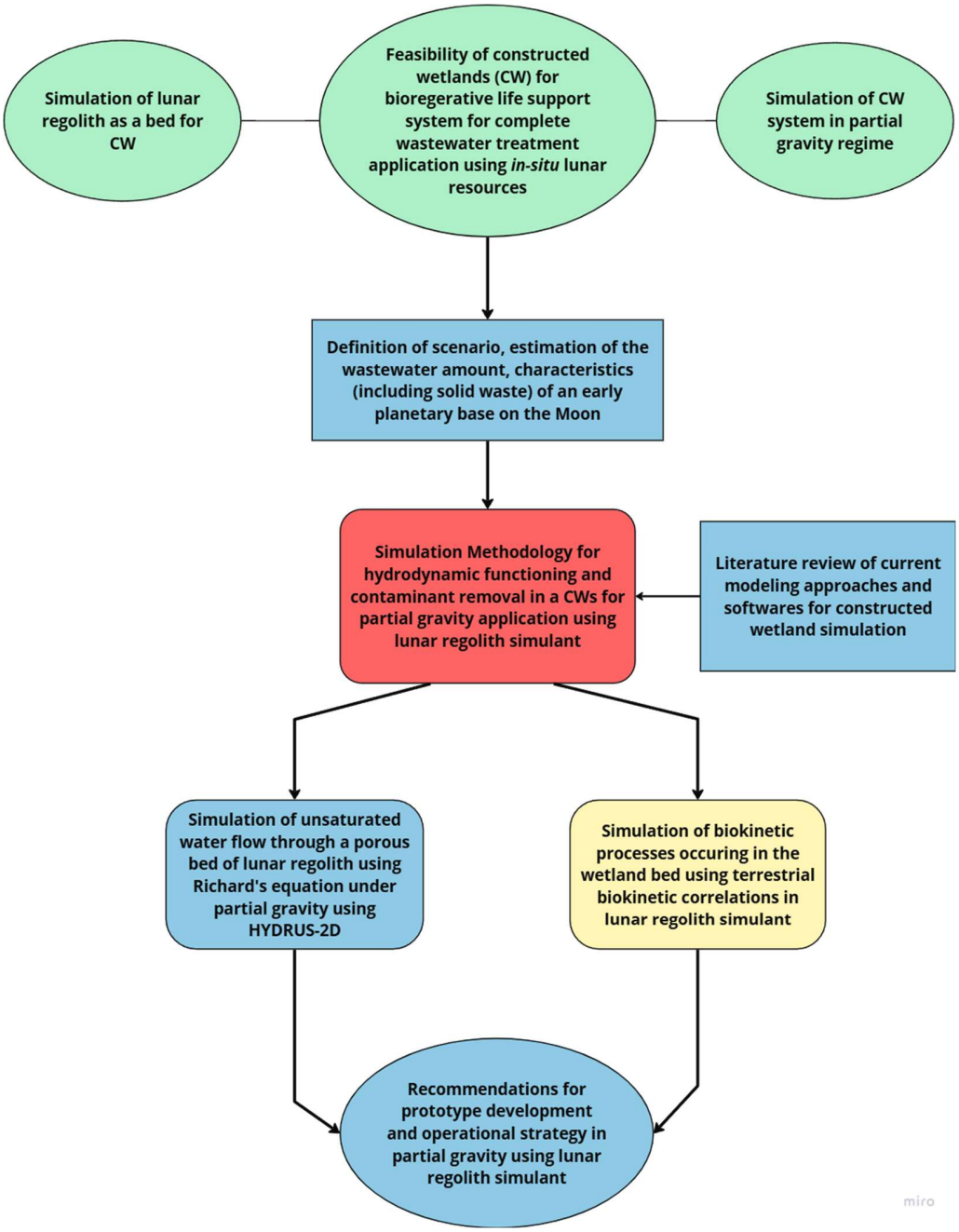

Figure 1.4: Figure shows the flow diagram for the research and simulation methodology used for achieving project objectives.

Chapter 2: Modeling framework and estimation of properties for VFCWs in partial gravity

2.1 Mathematical modeling of water dynamics through a porous bed

The wastewater flow through a soil or wetland substrate bed can be modeled as fluid flow through a porous bed. The porous bed in this study would be a particular substrate to be used in the ISRU context, such as lunar regolith. Although fluid flow through porous media has been widely studied by employing various modeling schemes, there are no studies that point out the flow in a partial gravity regime. The flow through a porous bed was first described by the French engineer Henry Darcy in his 1856 work titled *"Les Fontaines publiques de la ville de Dijon"* (The Public Fountains of the City of Dijon). It is governed by Darcy's law, which states that the velocity of flow through porous media (Q) is directly proportional to the hydraulic gradient ($\frac{\delta\Psi}{\delta z}$) for any given saturated soil under steady laminar flow conditions[49] which is analogous to Fick's law but for water in porous bed, which is expressed in mathematical form in Bonan et al., 2019[50] as follows:

$$Q = -K(\theta)\frac{\partial(\Psi + \mathrm{z})}{\partial z} = -K(\theta)\left[\frac{\partial\Psi}{\partial z} + 1\right] \tag{2.1}$$

$$Q = -K(\theta)\frac{\partial\Psi}{\partial z} - K(\theta) \tag{2.2}$$

where θ is the volumetric water content, Ψ is the matric potential, the pressure with which water is held in the substrate matrix due to the attraction between water molecules and porous particles ($\Psi < 0$) for unsaturated soil and ($\Psi \geq 0$) for fully saturated soil with liquid, z *i*s the height above the ground or reference point, and Q is the velocity of flow and has units of m^3/m^2.s. $K(\theta)$ is the hydraulic conductivity of the soil which describes how easily water can flow through it, and is dependent on volumetric water content (θ), which is the ratio of volume of water retained in the bed to the total volume of the bed. However, Darcy's law needs to be further modified to model the hydrodynamics of water in ecological processes, specifically in unsaturated conditions, also described in Bonan et al., 2019[50].

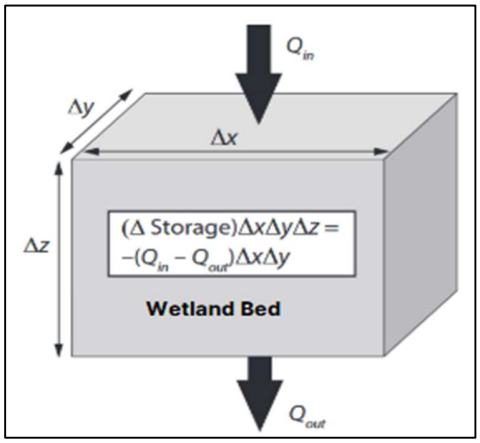

Figure 2.1.1: Figure shows the block diagram for mass balance on water movement through a wetland bed as shown in Bonan et al., 2019.

This modification of Darcy's law can be done by applying the continuity equation[50] on the wetland bed as shown in Figure 2.1.1, where Q_{in}, Q_{out} are the volume of wastewater entering and leaving the wetland bed respectively, assuming a cubic system where Δx, Δy, Δz are the dimensions of the bed, and observing the principles of mass conservation, the final equation is shown below:

$$\frac{\partial\theta}{\partial \boldsymbol{t}} = \frac{\partial}{\partial z}\left[K(\theta)\frac{\partial\Psi}{\partial z} + K(\theta)\right] \tag{2.3}$$

$$\frac{\partial\theta}{\partial \boldsymbol{t}} = \frac{\partial}{\partial z}\left[K(\theta)\frac{\partial\Psi}{\partial z}\right] + \frac{\partial \mathrm{K}}{\partial z} \tag{2.4}$$

Which is also called Richard's equation (3.3), with two independent variables ψ and θ, this equation can be written in terms of one independent variable, either as a function of θ or ψ.

$$C(\Psi)\frac{\partial\Psi}{\partial \boldsymbol{t}} = \frac{\partial}{\partial z}\left[K(\theta)\frac{\partial\Psi}{\partial z}\right] + \frac{\partial \mathrm{K}}{\partial z} \tag{2.5}$$

Where $C(\Psi) = \frac{\mathrm{d}\theta}{\partial\Psi}$ is called the specific moisture capacity (m^{-1})[50].

This form of Richards equation only depends on one independent variable (ψ) and can be utilized for saturated and unsaturated soil for the ground level and vadose zone (layer of soil and rock found just below the Earth's surface but above the groundwater table)[50]. However, since C(ψ) depends upon ψ, the equation is not mass-conserving when ψ changes over a discrete period. Therefore, Richard's equation can be further described in terms of dependence on the soil water content (θ):

$$\frac{\partial\theta}{\partial \boldsymbol{t}} = \frac{\partial}{\partial z}\left[D(\theta)\frac{\partial\theta}{\partial z}\right] + \frac{\partial \mathrm{K}}{\partial z} \tag{2.6}$$

Where, $D(\theta) = \frac{K(\theta)}{C(\Psi)}$ and is known as the hydraulic diffusivity ($m^2\ s^{-1}$).

2.1.1. Modeling of partial gravity using Richard's equation

Richards' equation is founded on relationships for K(θ) or θ(ψ), though analytical solutions are hard to find because these relationships are nonlinear. Numerical methods can normally be employed. Such methods initially create a finite difference form of the partial differential equation (PDE) and subsequently linearize the nonlinear terms containing K(θ) and C(ψ). The accuracy of the solution depends heavily on the specific numerical techniques used, the form of the Richards equation, and the time step and grid size used. Richard's equation is further expressed in three-dimensional form as follows:

$$Q = -K(\theta)(\nabla \mathrm{h} + \nabla \mathrm{z}) \tag{2.7}$$

Where the term (∇h + ∇z) represents the total head of the system from an arbitrary reference point. The effect of partial/lunar gravity in vertical motion in a porous bed can be estimated by using the correlation for the estimation of saturated hydraulic conductivity (K_{sat}) for lunar regolith in saturated conditions using the well-known Karmen-Cozeny predictive model[51] for K_{sat}, assuming a gravitational acceleration of 1.66 ms^{-2}.

$$K_{sat} = k\,(\frac{\rho g}{\eta}) \tag{2.8}$$

Where K_{sat} is the saturated hydraulic conductivity (ms^{-1}), k is the permeability (m^2), ρ is the liquid density [g/cm^3], g is the acceleration due to gravity (ms^{-2}), and η is the dynamic viscosity ($kg \cdot m^{-1} \cdot s^{-1}$). However, the Karmen-Cozeny predictive model is limited because it is based on Poiseuille's law for flow through a granular porous bed lacking structure or consolidation and is assumed to be a bundle of capillaries with a single representative radius. This approach works better with uniform pore size distribution.

2.1.2 Estimation of hydraulic parameters of wetland bed substrates

Richard's equation requires characterization of the hydraulic parameters of the porous bed media. The two main porous media simulated in this study are conventional wetland substrate (sand) and lunar regolith simulant (mare simulant (LMS-1)). In this study, the van Genuchten–Mualem model was used to characterize the unsaturated porous bed hydraulic properties. These properties are derived from the soil-water retention curve, which is often characterized empirically. The van Genuchten–Mualem model relates the volumetric water content (θ) to the pressure head (h)[52] as follows:

$$\theta(h) = \theta_r + \frac{\theta_s - \theta_r}{[1 + (\alpha h)^n]^m} \tag{2.9}$$

with h is the head and h > 0 and m = 1−1/n, the actual pressure head; θ (h) (m^3/m^3), the actual water content dependent on h; θ_r and θ_s (m^3/m^3), the residual and the saturated volumetric water contents respectively; α (1/m), the fitting scale and n (-), the shape parameter. The interpretation of these parameters is shown in Table 2.1.1. The van Genuchten–Mualem model parameters for the conventional wetland substrate (sand) are provided in the HYDRUS-2D database[53], and parameters for lunar regolith simulant (LMS-1) are already available in the literature[54]. The only commercially available lunar regolith simulant that has been characterized with the van-Genuchten model is LMS-1[54].

Table 2.1.1: The table shows the hydrodynamic parameters required in the van-Genuchten model

Parameter	Interpretation
θr (Residual Water Content) [-]	Minimum water content left in the bed after drainage
θs (Saturated Water Content) [-]	Maximum water content when the soil is fully saturated
α (Air Entry Suction Pressure) [1/cm]	Determines the pressure at which air enters the soil pores
n (Pore-size Distribution Parameter) [-]	Describes how uniform the pore sizes are
Ks (Saturated Hydraulic Conductivity) [cm/day]	The rate at which water moves through fully saturated soil
l (Pore Connectivity Parameter) [-]	Empirical parameter influencing hydraulic conductivity under unsaturated conditions

2.2 Mathematical modeling of contaminant transport/removal through a porous bed

Contaminant transport occurs simultaneously with the downward motion of wastewater in porous media such as VFCWs and involves complex mechanisms like advection, diffusion, and mechanical dispersion[55]. It is also evident that some contaminants or solutes move slower than the water passing through the bed, which needs to be modelled with an alternative approach. Solute transport is explained by the advection-diffusion equation, a one dimensional (1-D) form of which is shown below [56].

$$\frac{\partial C}{\partial \boldsymbol{t}} = D_L \frac{\partial^2}{\partial x^2} - v_x \frac{\partial C}{\partial x} - \frac{\rho_b}{\theta} \frac{\partial C^*}{\partial t} + \left[\frac{\partial C}{\partial t}\right]_{rxn} \quad (2.10)$$

Where each term of the equation describes the phenomena of dispersion, advection, sorption, and reaction respectively, where C is the concentration of solute in liquid phase (kg/m^3), t is the time (day), D_L is the longitudinal dispersion coefficient (m^2/day), v_x is the average linear groundwater velocity (m/day), r_b is the bulk density of the porous bed (kg/m^3), q is the volumetric moisture content or porosity for saturated media (unitless), C* is the amount of solute sorbed per unit weight of solid (no units) and rxn is the subscript indicating a biological or chemical reaction of the solute (other than sorption).

Other modeling approaches, such as single continuum models, can also represent contaminant transport in fractured porous formations for given conditions. However, these models require data on equivalent porosity and dispersion coefficients, typically determined through field experiments[57]. The integration of experimental data with a variety of modeling techniques, including coupled algorithms, has become increasingly popular in simulating the transport of contaminants and informing groundwater management [58]. CWs remove pollutants through settling, filtration, microbial degradation, adsorption, and plant interactions, effectively treating organics, nutrients, pathogens, heavy metals, and contaminants via integrated physical, chemical, and biological processes. When the solute transport involves chemical or biological reactions and microorganisms' growth, as the ones mentioned above, which is also the case in VFCWs, it is modelled as '**reactive transport**' [59].

2.2.1 Reactive transport modeling for VFCWs

Reactive transport modeling is an efficient tool for research on fluid migration and biogeochemical reactions in subsurface systems[60], and it also considers processes such as advection, diffusion, dispersion, and a number of reactions able to alter porous media properties[60]. These alterations lead to mechanisms of feedback that affect water flow, solute migration, and reaction rates[60] and, in turn, the removal of contaminants from the wastewater. Besides prediction, reactive transport modeling provides a conceptual framework for integrating experimental observations, comparing potential alternative biogeochemical processes, and identifying research needs[61]. The universality of the method makes it applicable in explaining complex interactions between transport and reaction processes in evolving porous media [60], which is utilized in a VFCW.

2.3 Modeling software review and selection

Richard's equation is a nonlinear PDE dependent upon the bed moisture content, which is a nonlinear function of head and hydraulic conductivity. Solving these nonlinear functions require an iterative approach since these parameters are coupled in such a way that they are dependent upon each other, and the equation cannot be decoupled into simpler parts. The equation is transient and cannot be solved for single time point and therefore require implicit or explicit methods like Euler or Crank-Nicolson, which is unstable or inaccurate without proper numerical schemes. For the above reasons, a numerical solver with advanced iterative techniques, matrix solver, and adaptive time stepping is required, for which a thorough software review was conducted with pros and cons in the context of application to VFCW and modifiable parameters. The results are summarized in Table A2 (Annex).

2.3.1 Modeling of hydrodynamic and contaminant removal using HYDRUS-2D

Among the various software reviewed, only a few of them are still currently available, among which the HYDRUS-2D model, which can be used for modeling variably saturated water dynamics and along with reactive transport of dissolved compounds, with an additional module for wetland kinetics (CW2D), which will be discussed in the next section. The HYDRUS-2D model solves Richards' equation using numerical methods and provides a graphic interface for the dynamics of water in a porous bed. HYDRUS provides variably saturated water flow results and estimates the hydrological properties with the van Genuchten model. The results can be obtained ranging from seconds to days. HYDRUS has both one-dimensional (HYDRUS-1D) and multi-dimensional (HYDRUS-2D/3D) versions, with the former being free and open-source but the latter being commercial[53]. The software has been under continuous development, with recent additions being specialized add-on modules that enhance its functionality [62]. HYDRUS can be used for direct and inverse problems, allowing for parameter estimation and model calibration by built-in optimization algorithms or by external global optimization methods. The models have been applied to a wide range of steady-state and transient flow and transport issues in field and laboratory situations[63].

Reactive transport can be modelled using HYDRUS-2D and has been enhanced considerably, allowing for the simulation of complex biogeochemical processes in subsurface systems and providing supporting experimental studies for parameter and data collection. Hydrus-2D has a specialized module for wetlands using two biokinetic models (CW2D and CWM1) for simulating CWs. CW2D module simulates solute transport, and organic matter, nitrogen, and phosphorus degradation by Monod-type equations and temperature-dependent rates using the activated sludge model [64]. The biological transformations considered in the CW2D module are described in S1 (Supporting Information). Reaction rate equations are shown in

Table A7 (Annex). CW2D has been applied in various applications, including wastewater treatment and combined sewer overflow (CSO) control[29,65]. Even though the model is effective for pilot-scale CWs, more research is needed to improve adsorption modeling, degradation processes, and influent fractionation for combined sewer overflow treatment[62]. The CW2D manual includes detailed information on the mathematical formulations of the module, default parameters that can be modified based on case information, and HYDRUS implementation, along with examples and additional input/output file descriptions [29].

2.3.2 Estimation of parameters for HYDRUS-2D simulation

Various parameters for contaminant transport modeling are required to validate the equation mentioned in the previous section for performing the reactive transport part simulation. Parameters such as longitudinal and transverse dispersion coefficients and initial solute concentrations (mentioned in the previous section) are estimated according to the substrate particle properties. Contaminant transport is simulated using the Crank-Nicholson time weighting scheme and Galerkin finite elements for spatial discretization[66,67]. The stability criterion is set to 2. Tortuosity is considered using the Millington & Quirk model[68]. Nonlinear adsorption is not a primary focus, as iteration criteria are minimal (tolerance values set to zero with one iteration). Twelve solute transport components shown can be modeled with a modifiable pulse duration (cm/day) and units of (mg/L) as shown in Table 2.3.1 below. Initial solute concentrations are defined in the liquid phase (mass of solute per volume of water), assuming equilibrium between phases at the start and the contaminants are modelled as dissolved in the influent wastewater. Additional modules (e.g., attachment/detachment) were not enabled.

In HYDRUS-2D CW2D module, the total COD is further distributed into **readily biodegradable** (rCOD), **slowly biodegradable** (sCOD), and **inert COD** (iCOD) for simulation of these components. The distribution can be seen in the Table 2.3.1 below by Langergraber and Simunek 2006[29]. The initial amount of microbial concentration in the bed and influent can also be assigned by changing the concentrations of the component 5 for heterotrophic species and 6,7 for autotrophic bacteria. The profile of microorganisms can be set by using the graphical interface and assigned concentration to the specific area of the bed according to supporting literature. Further parameters of contaminant transport in equation 3.5 like longitudinal and transverse dispersivities play an important role in the contaminant removal processes, the estimation of these parameters for lunar regolith can be done by using particle information mentioned in Slyuta et al., 2013[69] and shown in Table A3 (Annex) as explained in the next section.

Table 2.3.1: Table shows the twelve solute transport components that can be modelled in HYDRUS-2D

No.	Component	Symbol	Unit
1	Dissolved oxygen (DO)	O_2	$mgO_2\ L^{-1}$
2	Readily biodegradable COD	rCOD	$mgCOD\ L^{-1}$
3	Slowly biodegradable COD	sCOD	$mgCOD\ L^{-1}$
4	Inert chemical oxygen demand	iCOD	$mgCOD\ L^{-1}$
5	Heterotrophic microorganism	XH	–
6	*Nitrosomonas spp.* (autotrophic bacteria 1)	XAN_s	–
7	*Nitrobacter spp.* (autotrophic bacteria 2)	XAN_b	–
8	Ammonium ion (NH_4^+)	NH_4N	$mgN\ L^{-1}$
9	Nitrite ion (NO_2^-)	NO_2N	$mgN\ L^{-1}$
10	Nitrate ion (NO_3^-)	NO_3N	$mgN\ L^{-1}$
11	Dinitrogen gas (N_2)	N_2N	mg/L
12	Inorganic phosphorus	IP	mg/L

2.3.3 Estimation of the total COD in influent wastewater from an early planetary base

The influent composition of wastewater from an early planetary base differs from typical terrestrial domestic raw wastewater. Therefore, the components such as COD, NH_4^+, NO_2^- differ in these wastewaters. Since such wastewater formulation has not yet been present, to provide an initial estimation, influent flow rate and composition can be inferred from the Baseline Life Support Baseline Values and Assumptions Document (BVAD)[70], as well as data from ersatz formulations[71]. With an assumption that organic matter, such as feces and urine, has a similar COD value to that in earthly conditions, and is mixed in the toilet flush. The wastewater is mixed with latent wastewater, which is the crew's latent humidity generated purely due to latent heat processes from the crew's respiration, perspiration, and other activities in a closed environment. Further distribution of wastewater in BVAD is shown in Table A4 (Annex).

According to the BVAD, each crew member should generate about 32 g of feces dry matter per day and 1.56 kg of urine per day. Correlating this dry matter to COD by using empirical values tested on earth, which corresponds to the dry matter of feces and urine to corresponding COD value which comes out to be 63495 mg in total, when this is divided by the total flush water volume (2.2334 L assuming density of water), we can get the resulting COD as 28429.7 mg/L in the flush water which is 22.3% of the total wastewater according to the BVAD, which gives us the final COD of 6328.46 mg/L after dilution.

Furthermore, Verostko et al., 2004[71] attempted to formulate the wastewater in an early planetary base and did some empirical measurements of the total carbon content (TOC), which is shown to be 519 - 631 mg/L as shown in Table A5 (Annex). A correlation between COD and TOC is shown in Figure A2 (Annex). Using this correlation and assuming again the wastewater composition like that of terrestrial wastewater, we can estimate that the COD value ranges from (6725.91 - 8158.73 mg/L).

For an initial estimate, a 50% COD removal was assumed in the septic tanks owing to settling. Septic tanks are generally used as a reservoir for storing wastewater prior to the treatment and can function without intervention for a long time[72]. A final total COD value of 3000 mg/L was taken as a basis for the simulation study. This estimated COD is comparable to industrial wastewater rather than domestic wastewater. This value provides an initial estimate for influent concentrations defined in the methodology which are expected to be revised once empirical data is available from the prototyping phase.

2.4 Simulation of operational strategies

Different operation modes and feeding strategies can be employed for the proper operation and contaminant removal in a VFCW as discussed in Section 1.2.3, some of which have been well-established such as CFS and IFS. These operational strategies are of interest in this study due to time, substrate and spatial constraints. Furthermore, these strategies that require little to no extra machinery and moving parts are preferred in the context of this study. The objectives of the treatment system can be met by focusing on key performance indicators such as contaminant removal efficiency (e.g., COD, nitrogen, phosphorus), effluent quality, saturation time, space efficiency, and system complexity.

The HYDRUS-2D software can further be employed to simulate these operational scenarios under partial gravity **by changing the feeding time** and the schedule and **frequency of feeding wastewater**. Such versatile model simulation results for a VFCW using these different feeding strategies, substrates and gravity conditions could be determining key parameters of focus. These scenarios can also be evaluated based on their effectiveness in pollutant removal primarily COD removal and nitrate in the effluent. These simulation results will help aid the resource requirements, operational feasibility, and adaptability in the context of space exploration and use in area deficient countries.

Chapter 3: Methodology & Simulation Parameters

3.1 System setup

The geometry of the modelled system is an axis-symmetrical cylinder with dimensions of a radius of 50 cm and a height of 100 cm, containing a single substrate porous bed. The simulation was performed using HYDRUS-2D version 5.05 with the CW2D wetland module as an additional module for the simulation of reactive transport. The substrate bed is modelled by using the Finite Element Mesh method[73], using a maximum of 500000 mesh nodes for observation of fluid flow, as shown in Figure 3.1.1. The hydrodynamics in the VFCW bed was simulated under Earth and partial gravity conditions using sand and lunar regolith simulant (Lunar Mare Simulant (LMS-1)) as a substrate medium for comparison.

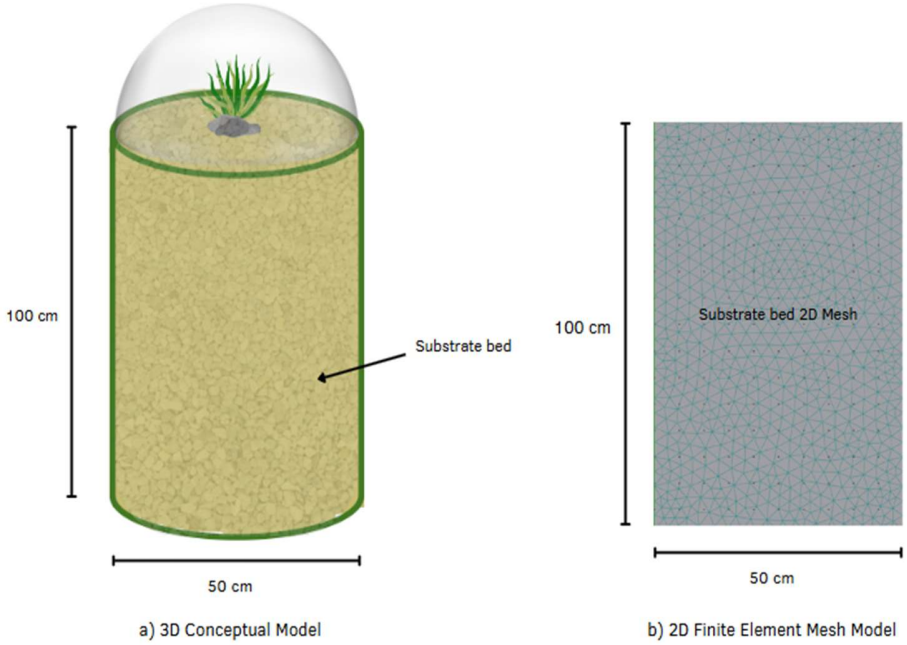

Figure 3.1.1: Figure shows the 3D conceptual model (a) and 2D finite element mesh model (b) constructed on HYDRUS-2D.

3.2 Model assumptions

The model assumptions are described below:

- The system was modeled as a two-dimensional axisymmetric domain.
- Flow and solute transport were assumed to be predominantly vertical; lateral movement was considered negligible.
- The filter media (sand and lunar regolith simulant) were treated as hydraulically and physically homogeneous.
- A constant ambient temperature of 20 °C was assumed, reflecting a climate-controlled indoor environment on Earth or the Moon.
- Gravity was varied between Earth (9.81 m/s²) and Moon (1.62 m/s²), while:
- Microbial kinetics and reaction rates in CW2D were assumed not to vary with gravity.
- The surface was exposed to aerobic atmospheric conditions.
- The system was assumed to be unplanted, with negligible evapotranspiration.
- CW2D modeled organic matter and nitrogen transformations, but did not account for, pH changes, redox potential variations, or salinity effects.

3.3 Simulation settings & initial conditions

At initial conditions of hydrodynamics, the bed is at field capacity (having enough available water for plant growth), which can be modified based on the substrate media. It is the amount of residual moisture in the soil when the soil is dry/nonsaturated. This was estimated to be a head of -93.347 m throughout the bed in HYDRUS-2D. The effect of partial gravity was simulated as discussed in Section 2.1.1 (Equation 2.7 & 2.8). The microorganism profile in the porous bed was selected based on Lagergraber & Tietz 2007[74] as shown in Table 3.3.1. The bed has a gradient of heterotrophic microorganisms 500 mg/L reducing to zero at 50 cm of the bed, while the bed contains 30 mg/L of autotrophic bacteria (*Nitrosomonas spp.)* reducing from the top of the bed to the lowest depth as 0 mg/L and 15 mg/L of autotrophic bacteria (*Nitrobacter spp.*) starting from the top of the bed and decreasing linearly to 0 mg/L at lowest time as shown in Table 3.1.1.

Table 3.3.1: Table shows the assumed microorganism profile in the bed using HYDRUS-2D based on empirical data in Lagergraber & Tietz 2007[74] and Wetland Example 1[75]

Microorganism Type	Bed Depth	Concentration
Heterotrophic microorganisms	1-50 cm	Linear decrease from 500 mg/L to 0 mg/L
Autotrophic bacteria	1-100 cm	Linear decrease from 30 mg/L (*Nitrosomonas spp.)* and 15 mg/L (*Nitrobacter spp.*) to 0 mg/L

The kinetic parameters used in the simulation were based on the CW2D module mentioned in Table A6 (Annex). The simulation was configured with an initial time step of 0.0001 day, and an observation interval of 1 day. To ensure numerical stability and accurate resolution of transient processes the maximum number of iterations were set to 100 for hydrodynamic simulation and 10 for solute transport simulation. The total simulation duration (minimum 10 days and maximum 60 days) was set to adequately capture the system at saturated performance and provide enough time to observe contaminant removal or accumulation while reducing computing time. The results for effluent concentrations were taken directly at the seepage end of the bed.

3.4 Hydraulic & solute transport properties of substrates

For the van-Genuchten model, hydraulic parameters were taken from Brozovich et al., 2024[54] particularly relating to the Lunar Mare Simulant (LMS-1) and for sand the parameters were taken directly from HYDRUS database as shown in Table 3.4.1. The solute transport parameters for sand were taken directy from the HYDRUS database. The longitudinal dispersion coefficient D_L in lunar regolith was estimated using the relation $D_L=\alpha_L \cdot v$, where αL is the longitudinal dispersivity and v is the average seepage velocity. Based on particle size distribution data from Slyuta et al. (2014)[69] (Table A3, Annex), the mean grain size was approximated as 0.01 cm. Assuming a seepage velocity of 3 cm/day[76], the dispersivity coefficient was calculated as $D_L=0.015\ cm^2/day$. This gives a corresponding longitudinal dispersivity of 0.005 cm. This parameter is crucial, as dispersivity is influenced by grain size, which affects pore structure and solute transport pathways in the regolith.

To estimate the transverse dispersion coefficient D_T in lunar regolith, the formula $D_T=D_m+\alpha_T v$ is used, where D_m is the molecular lateral diffusion coefficient (negligible for lunar soils as predominant motion is vertical in the setup), α_T is the transverse dispersivity, and v is the seepage velocity. Assuming lateral negligible diffusion, $D_T \approx \alpha_T v$. An empirical relationship $D_T=\phi K$ is applied, where ϕ is the porosity (44%) and K is the hydraulic conductivity (13.34 cm/day), resulting in $D_T=5.87\ cm^2/day$. Using

v=3 cm/day, the transverse dispersivity is then calculated as α_T=1.96 cm. Understanding transverse dispersivity is essential for modeling lateral solute spread in porous media such as lunar regolith. Other solute-specific parameters, such as the molecular dispersion coefficient of solutes in different media, were used based on the HYDRUS dataset[75] as shown in Table 3.4.2 and Table A7 (Annex).

Table 3.4.1: Table shows the list of hydraulic parameters derived from van-Genuchten model for solving Richard's equation in HYDRUS-2D

Substrate	θr (Residual Water Content) [-]	θs (Saturated Water Content) [-]	α (Air Entry Suction) [1/cm]	n (Pore-size Distribution Parameter) [-]	Ks (Saturated Hydraulic Conductivity) [cm/day]	l (Pore Connectivity Parameter) [-]
Sand (HYDRUS database)	0.045	0.43	0.145	2.68	712.8	0.5
Lunar regolith Simulant (LMS-1) (Brozovich et al., 2024)	0.0651	0.3098	0.02 (taken for silty loam Hydrus database)	4.092	13.34	0.5

Table 3.4.2: Table shows a comparison is shown between the solute transport parameters used for sand compared to lunar regolith simulant (LMS-1).

Substrate	Mean Grain Size	Bulk Density	Porosity (ϕ)	Longitudinal Dispersivity (α_L)	Transverse Dispersivity (α_T)	Saturated Hydraulic Conductivity (K_{sat})
Sand (HYDRUS database)	0.063-2 mm	1.5 g/cm^3	0.37-0.46	0.5	0.1	712.8 cm/day
Lunar Regolith (Estimated)	0.1 mm	1.5 g/cm^3	0.44	0.005 cm	1.96 cm	13.34 cm/day

3.5. Influent contaminant concentrations

The concentrations of different components present in the influent are shown in Table 3.5.1. The values were taken as an initial estimate using the COD estimate done in the Section 2.3.3(3000 mg/L) and Wetland Example 1 (HYDRUS Manual). The COD was distributed into a rCOD, sCOD, and iCOD based on the distribution in HYDRUS manual. The assumed concentrations are to be revised once empirical data is acquired from the prototyping phase of the project. The formula used for calculation of the COD removal (%) is as follows.

$$Percentage\ removal\ (\%) = \frac{Influent\ Concentration - Effluent\ Concentration}{Influent\ Concentration} \times 100$$

Table 3.5.1: The table shows the concentrations of different components present in the influent wastewater used in the simulation

Component	Symbol	Value	Unit	Reference
Dissolved oxygen (DO)	O_2	0.282	mg/L	Jelena 2023
Readily biodegradable COD	rCOD	1600	mg/L	BVAD, Langergraber & Simunek 2006
Slowly biodegradable COD	sCOD	1200	mg/L	BVAD, Langergraber & Simunek 2006
Inert COD	iCOD	200	mg/L	BVAD, Langergraber & Simunek 2006
Heterotrophic microorganism	XH	500	mgCOD/L	Assumption
Nitrosomonas spp. (autotrophic bacteria 1)	XANa	20	mgCOD/L	Assumption
Nitrobacter spp. (autotrophic bacteria 2)	XANb	15	mgCOD/L	Assumption
Ammonium ion (NH_4^+)	NH4N	50	mg/L	Langergraber & Simunek 2006
Nitrite ion (NO_2^-)	NO2N	3	mg/L	Langergraber & Simunek 2006
Nitrate ion (NO_3^-)	NO3N	30	mg/L	Langergraber & Simunek 2006
Dinitrogen gas (N_2)	N2N	0	mg/L	Langergraber & Simunek 2006
Inorganic phosphorus	IP	116	mg/L	Shrestha et al., 2023[77]

3.6. Optimization and sensitivity analysis

The main operation scenario was based on a four-person astronaut base producing 40 kg of maecerated wastewater per day, which was taken as the basis for the initial water dynamic results and feasibility for the bed to process 40 L wastewater/day from a 4-person astronaut base. Further strategies of operation explored in CFS strategy to meet the 40L/day requirement in partial gravity using lunar regolith simulant. A comparison was made between different feeding schedules by increasing the frequency of feeding and decreasing the amount of wastewater added to obtain an **optimized CFS** strategy for water dynamics. Then contaminant removal was checked for this optimized CFS scenario and an alternative operation scheme using IFS was developed by trial and error until the required removal rate of pollutants was achieved in both lunar and earth gravity using conventional substrate (sand) and lunar regolith simulant

Table 3.6.1: Table shows the rationale for comparison of different cases for determining simulation strategy.

Substrate and Condition	Sand	Lunar Regolith
Earth Gravity	For validation of the results of simulation	For comparison between conventional substrate and ISRU substrate and validation of result
Partial Gravity	Checking for the effect of partial gravity on functioning of VFCW	Determining optimized hydrodynamic and nutrient removal strategy for a VFCW implemented on the moon with in-situ resources

---

Chapter 4: Results & analysis

The structure of the results and analysis is broken down into two parts, results of the water dynamics and results of the contaminant removal. The results of water dynamics were taken as a basis for checking contaminant removal as shown in Figure 4.0.1.

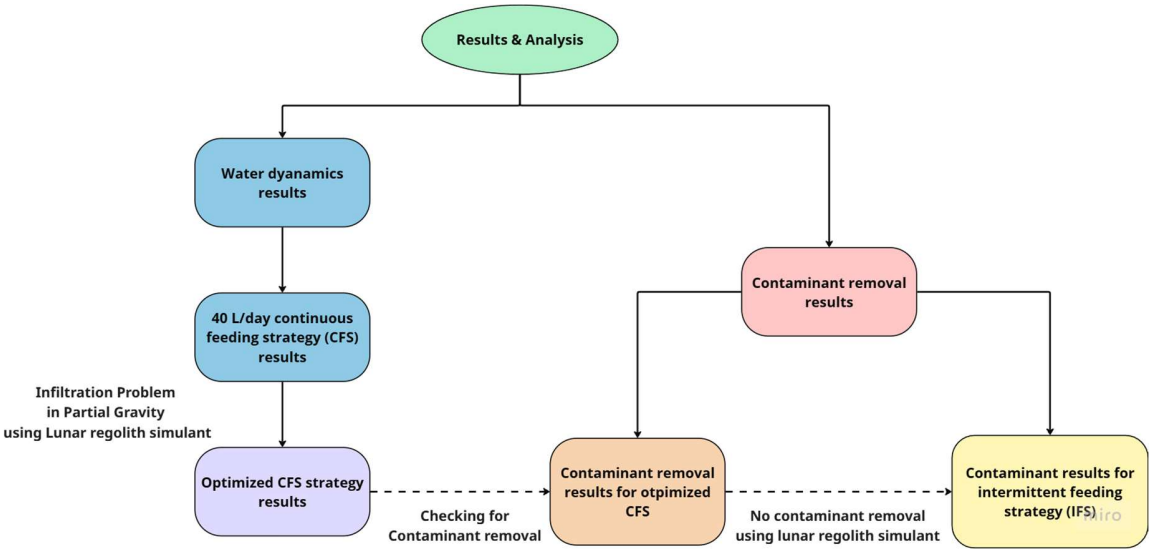

Figure 4.0.1: Figure shows the flow of the results of simulation using HYDRUS-2D for water dynamics and contaminant removal.

4.1 Simulation results of water dynamics through substrate bed

4.1.1. Simulation results of water dynamics through substrate bed using 40L/day CFS

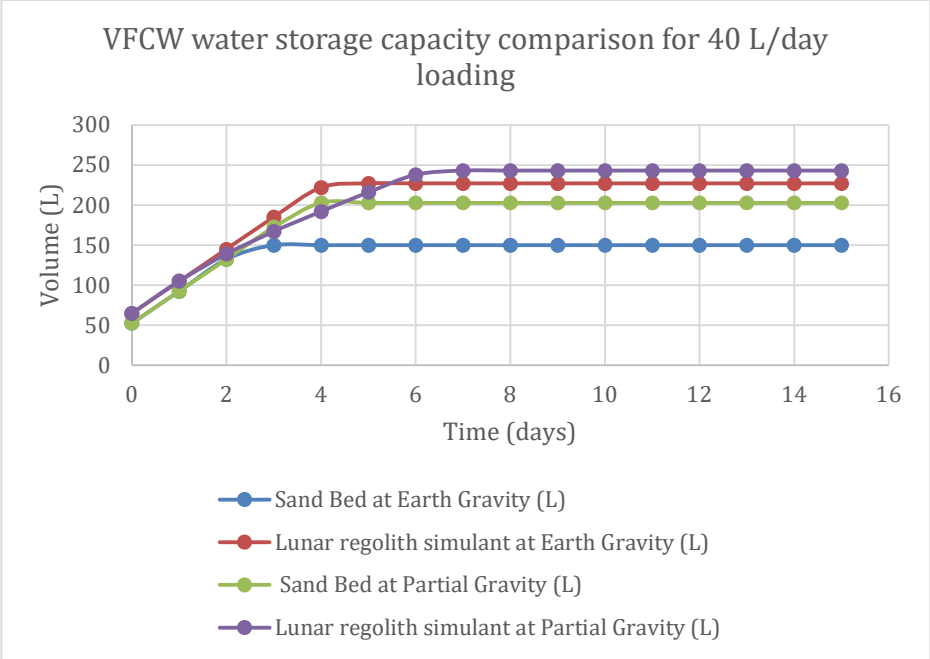

Figure 4.1.1: Figure shows the simulation results from HYDRUS-2D for comparison of bed water storage for different substrates (sand & lunar regolith simulant) in different gravity conditions for a 15-day simulation for hydrodynamics (40L/day loading).

The water volume retained in the bed was simulated by the addition of 40 L of wastewater over the bed once every 24 hours, which is the expected wastewater load in a 4-person astronaut base. The simulation results shown in Figure 4.1.1 shows the comparison of the two substrates (sand and lunar regolith simulant) in partial and earth gravity conditions. As it can be observed the sand bed substrate shows less tendency to accumulate water in its pores compared to lunar regolith simulant, further, it shows even lower water retention in the bed in earth gravity compared to partial gravity.

Compared to sand substrate, lunar regolith simulant shows lower sensitivity to gravity and a difference of bed water storage. Another important parameter shown in Figure 4.1.1 is the saturation time (how fast the bed reaches steady-state or saturated conditions) and this time is the slowest (6 days) for lunar regolith simulant in partial gravity compared to other substrates which reach steady state in lower time (around 4 days for sand).

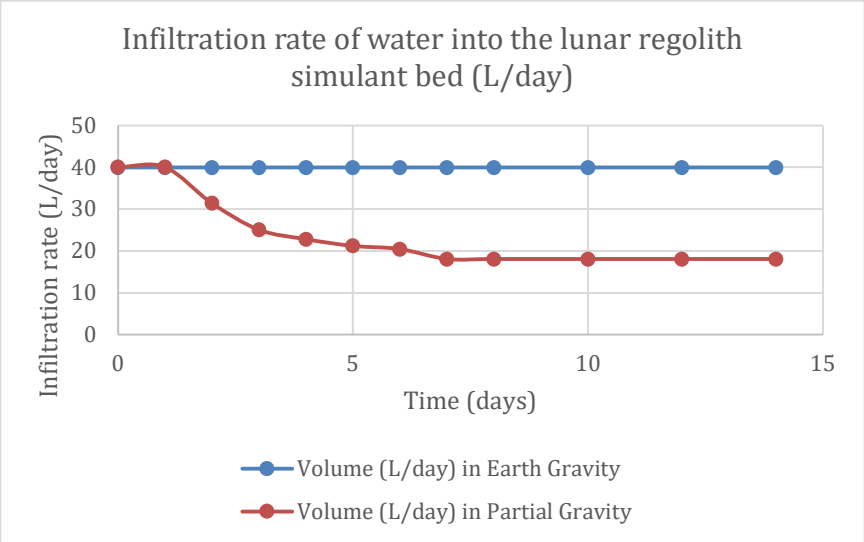

Figure 4.1.2: Figure shows the simulation results from HYDRUS-2D for infiltration rate of wastewater into the lunar regolith simulant bed in earth and partial gravity for the 15-day simulation for hydrodynamics (40/L day loading)

Using 40 L/day wastewater feeding method should complete the requirement of the base however, checking the infiltration rate shown in Figure 4.1.2, which shows how much water infiltrates through the bed over a certain time, it can be observed that the infiltration rate decreases over time in partial gravity compared to earth gravity. The decrease in infiltration rate occurs over the first 8 days after which the infiltration rate reaches 19 L/day. This is almost half of the infiltration rate required for functioning. Compared to sand bed and earth gravity conditions, this is the only case that causes surface accumulation/runoff as shown in Figure 4.1.5.

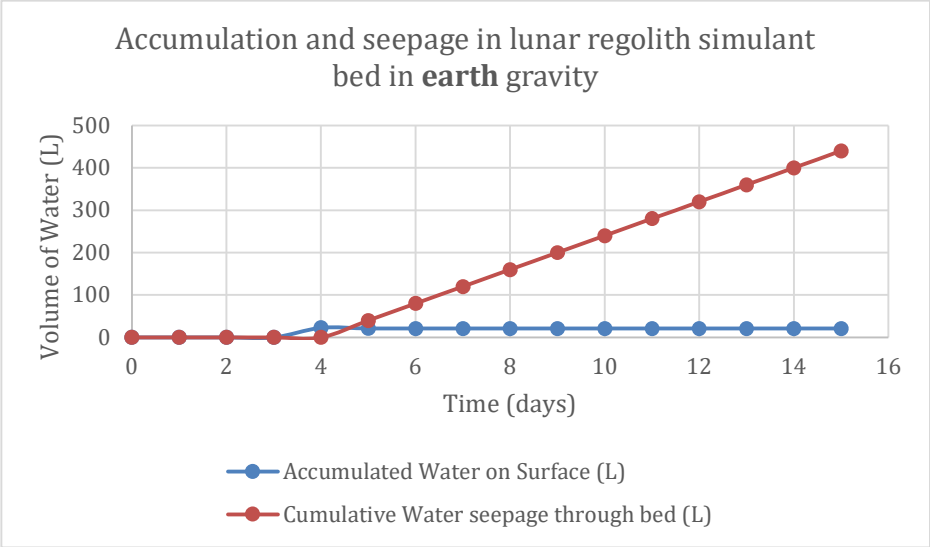

Figure 4.1.3: Figure shows the simulation results from HYDRUS-2D for accumulation of wastewater on the lunar regolith simulant bed and seepage out of the bed in earth gravity for the 15-day simulation for hydrodynamics (40L/day loading).

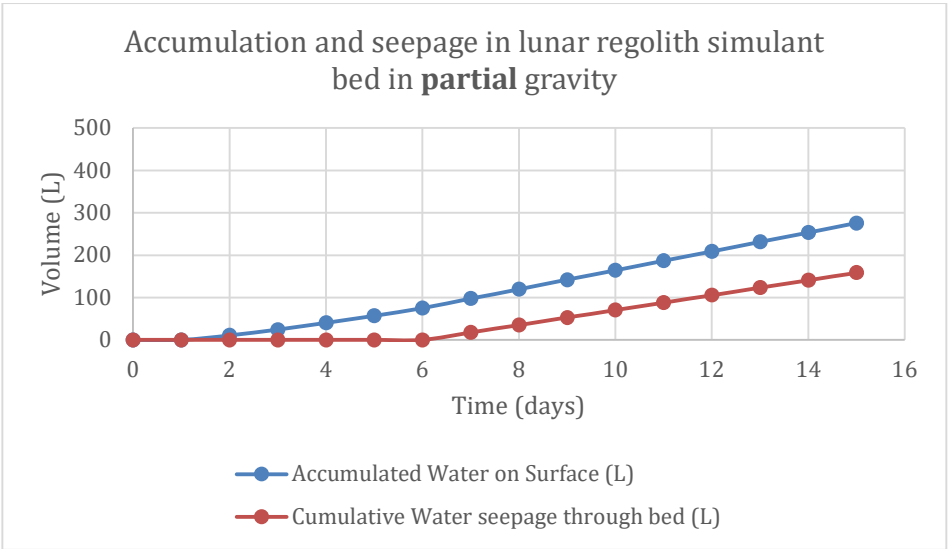

Figure 4.1.4: Figure shows the simulation results from HYDRUS-2D for accumulation of wastewater on the lunar regolith simulant bed and seepage out of the bed in partial gravity for the 15-day simulation for hydrodynamics (40L/day loading).

As can be observed in Figure 4.1.3, the lunar regolith simulant in **earth** gravity shows a constant level of initial accumulation of water on top of the bed after four days. These results show a manageable accumulation (<20 L) as the seepage of water through the bed reaches a steady rate on day 5. However, Figure 4.1.4 shows that in **partial** gravity accumulated water keeps increasing as with the seepage. The

seepage of water is not enough to balance out the accumulated water being accumulated on top, which is simulated as surface runoff, shown in Figure 4.1.5. This provides a major problem in the working of the system, since eventually the system exceeds the headspace/freeboard height of the bed and causing spill over. This is an operational disruption in the working of the system, especially in the context of limited spatial constraints.

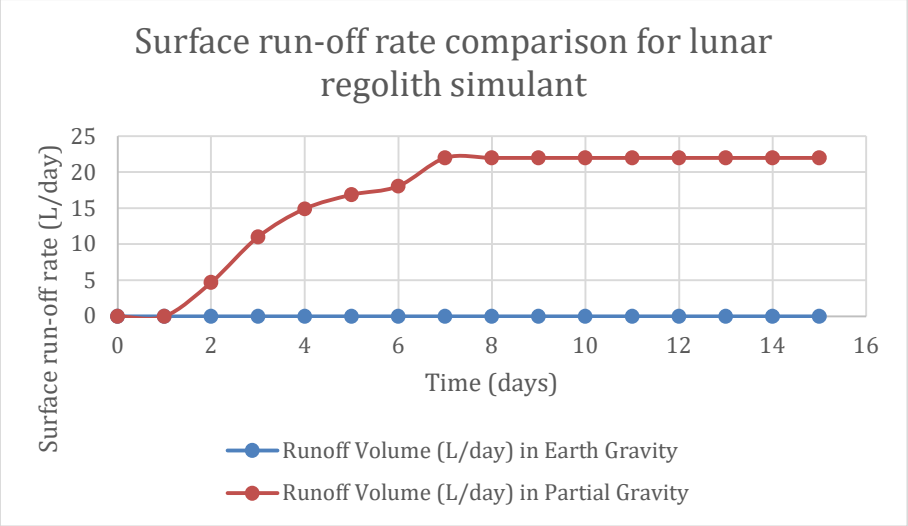

Figure 4.1.5: Figure shows the simulation results from HYDRUS-2D for comparison of surface run-off in lunar regolith simulant bed in earth and partial gravity for 15-day hydrodynamic simulation (40L/day loading).

4.1.2. Simulation results of water dynamics through substrate bed using optimized CFS

To eliminate this operational disruption with spatial constraints in lunar base context, different operation strategies could be implemented, mainly to optimize for no surface run-off/accumulation on top of lunar regolith bed in partial gravity. Different feeding times (hours) were checked with combination of volumes (liters) of wastewater added on the bed to come up with a feeding technique which does not show this problem. The results of these simulation trials are summarized in Table 4.1.1. Apart from surface run-off, the time taken for the bed to reach steady/saturated state (saturation time) is also an important parameter in this context as it tells how much time would be required for starting the system. Higher saturation times can be unfavorable however, optimizing for lower surface run-off correlates to addition of lower volumes of wastewater/time. This further reduces the rate at which water passes through the bed upto 14 days.

From table 4.1.1, the strategy which allows for lowest surface runoff rates (0 L/day) is addition of around 12 L of wastewater added per 7 hours. This strategy provides no runoff but also passes 40 L wastewater per day. Therefore this strategy is the **optimized continuous feeding strategy (CFS)** for lunar

regolith simulant bed in partial gravity. The results of optimized CFS are displayed below in figure 4.1.6. and 4.1.7.

Table 4.1.1: Table shows the simulation results from HYDRUS-2D for optimization trials for wastewater feeding strategies tested in partial gravity using lunar regolith simulant for zero surface run-off

Condition	Volume (L)	Feeding Time (hours)	Saturation time (days)	Surface run-off/Accumulation occurred (L/day)
1	11.8	7.2	14	0
2	19.9	12	9.5	2.4
3	23.6	14.4	7.5	5.9
4	39.3	24	6	22.3
5	80	48	6	62.8

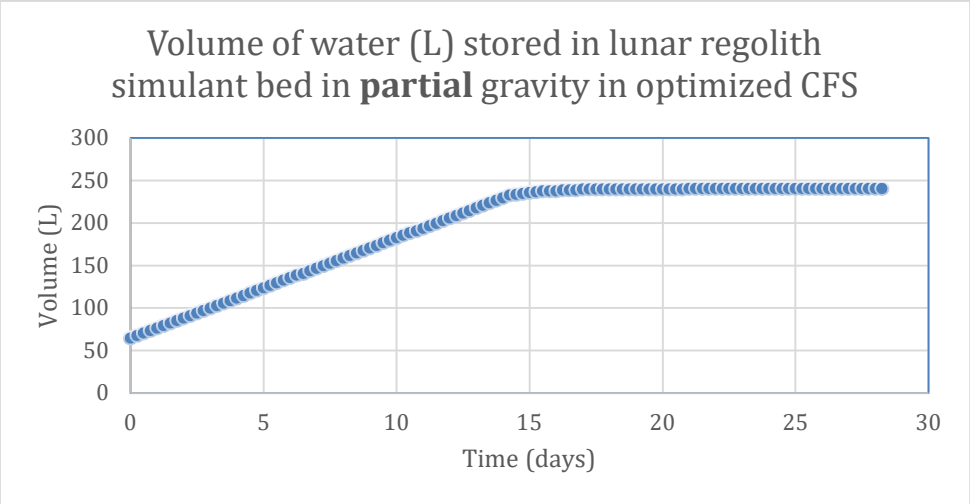

Figure 4.1.6: Figure shows the simulation results from HYDRUS-2D for the volume retained in lunar regolith simulant bed at partial gravity using optimized CFS (11.8 L every 8 hours) for lower surface runoff/accumulation of wastewater.

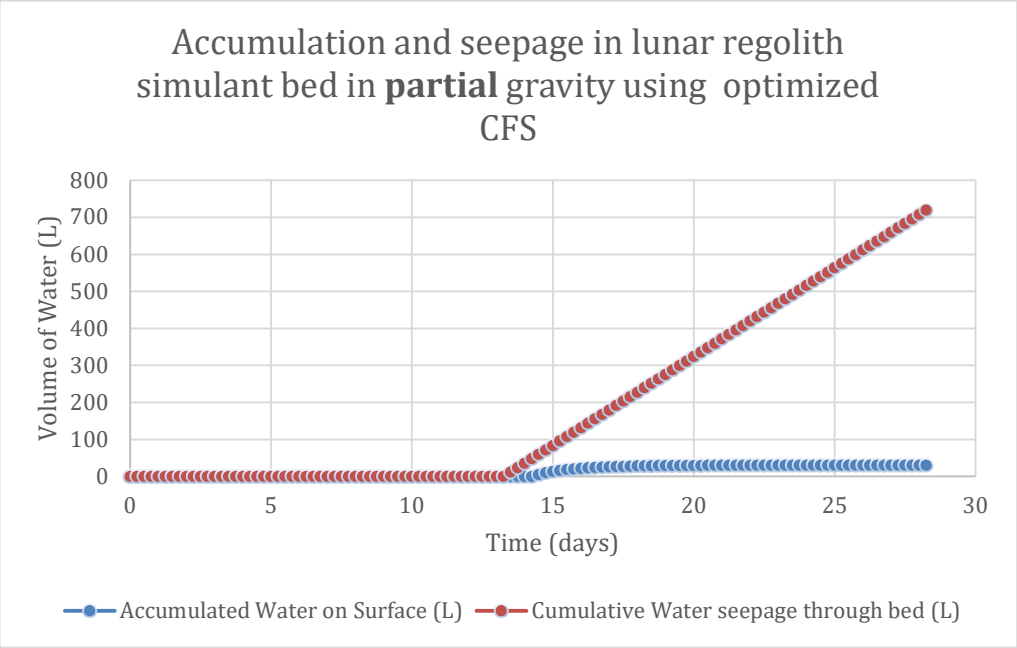

Figure 4.1.7: Figure shows the simulation results from HYDRUS-2D for water retained in lunar regolith simulant bed at partial gravity using optimized CFS for lower surface runoff/accumulation of wastewater.

Figure 4.1.7 illustrates that the optimized water balance results in CFS shows a lower accumulation compared to Figure 4.1.4 in partial gravity, where the feeding strategy was 40 L/day added at one instance. The breaking down of feeding volume into smaller doses in smaller interval, helped reduce the accumulation of water over the substrate in partial gravity. However, as discussed earlier, this increased saturation time from 6 days to 14 days. For conventional substrate (sand), this problem does not arrise in partial or earth gravity, therefore, the exploration of optimization strategies are not needed. This issue was also **not** observed in the lunar regolith simulant under **Earth** gravity, showing that the root cause of this problem could be the decrease in gravity and the hydraulic properties of lunar regolith simulant. In the next section the contaminant removal was checked in this optimized CFS strategy.

4.2 Simulation results of contaminant removal

4.2.1 Simulation results for contaminant removal using optimized CFS

The optimized CFS for lunar regolith simulant bed in partial gravity was taken as a basis for simulating the contaminant removal and the simulation results are summarized in tables and figures below. The Table 4.2.1 describes the effluent concentrations received by using the optmized CFS (~11.8L of wastewater added every 7-8 hours).

Table 4.2.1: Table shows the results of 30th day contaminant removal for sand and lunar regolith simulant substrate bed using CFS (11.8 L of wastewater added every 0.25 days) in earth and partial gravity conditions

Component	Gravity	Substrate			
		Sand		Lunar regolith simulant (LMS-1)	
		Earth	Lunar	Earth	Lunar
	Influent	Effluent			
Readily biodegradable COD (mg/L)	1600	1.05	0.94	1031	1420
Slowly biodegradable COD (mg/L)	1200	8.67	6.32	505.65	526.3
Inert COD (mg/L)	200	532.9	533.89	203.4	189.09
Ammonium ion (NH_4^+) (mg/L)	50	0.017	0.02	23.72	42.52
Nitrite ion (NO_2^-) (mg/L)	3	0.001	0.001	0.56	0.02
Nitrate ion (NO_3^-) (mg/L)	30	31.77	30.17	9.77	0.26
Dinitrogen gas (N_2) (mg/L)	0	20.92	23.56	73.77	81.23
Phosphorus (inorganic) (mg/L)	116	3.02	3.34	6.51	7.64

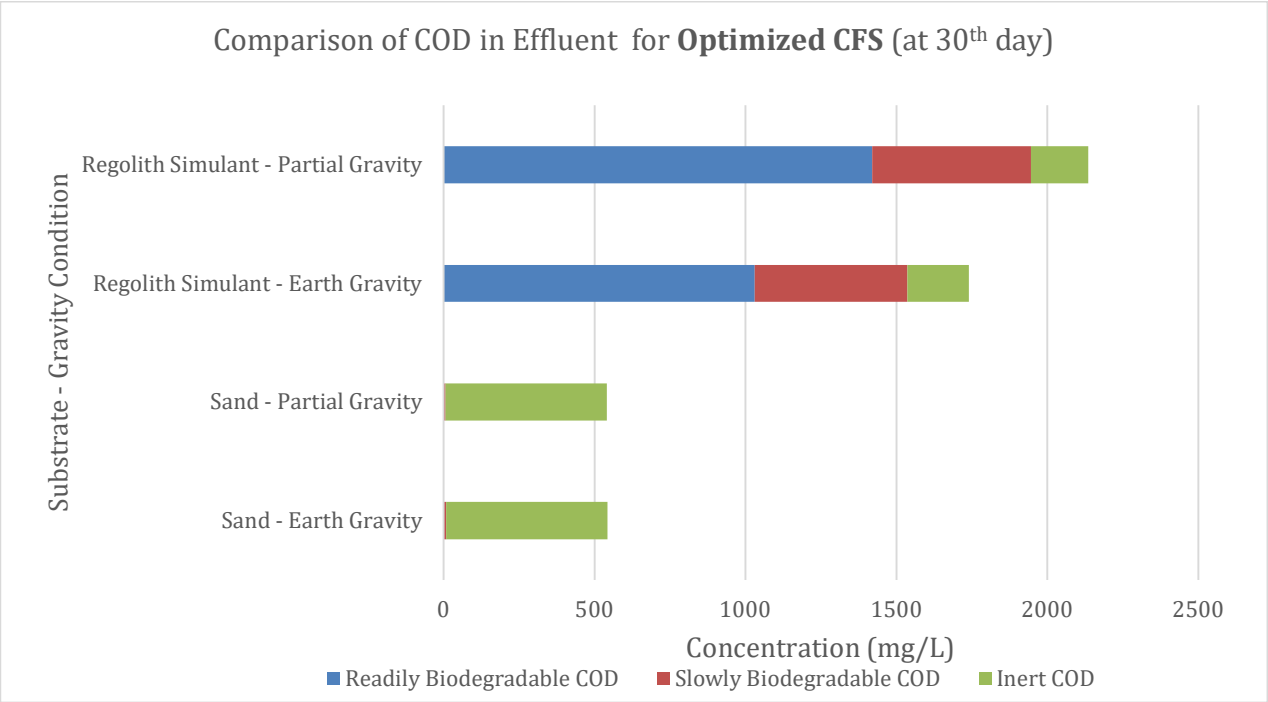

Figure 4.2.1: Figure shows the comparison of COD distribution in effluent at 30th day in optimized CFS for different substrates and gravity conditions.

It can be inferred through Table 4.2.1 that the total COD removal (%) is comparably higher in sand (81.9% in both earth and partial gravity) than lunar regolith simulant (52.5% in earth gravity and 14.9% in partial gravity). Furthemore, Figure 4.2.1 shows that sand removes most if not all of the rCOD and sCOD present in the influent but accumulates more iCOD, also known as sludge, however, lunar regolith simulant does not retain as much of the sludge (iCOD) as sand, allowing for lesser need for sludge removal in long term.

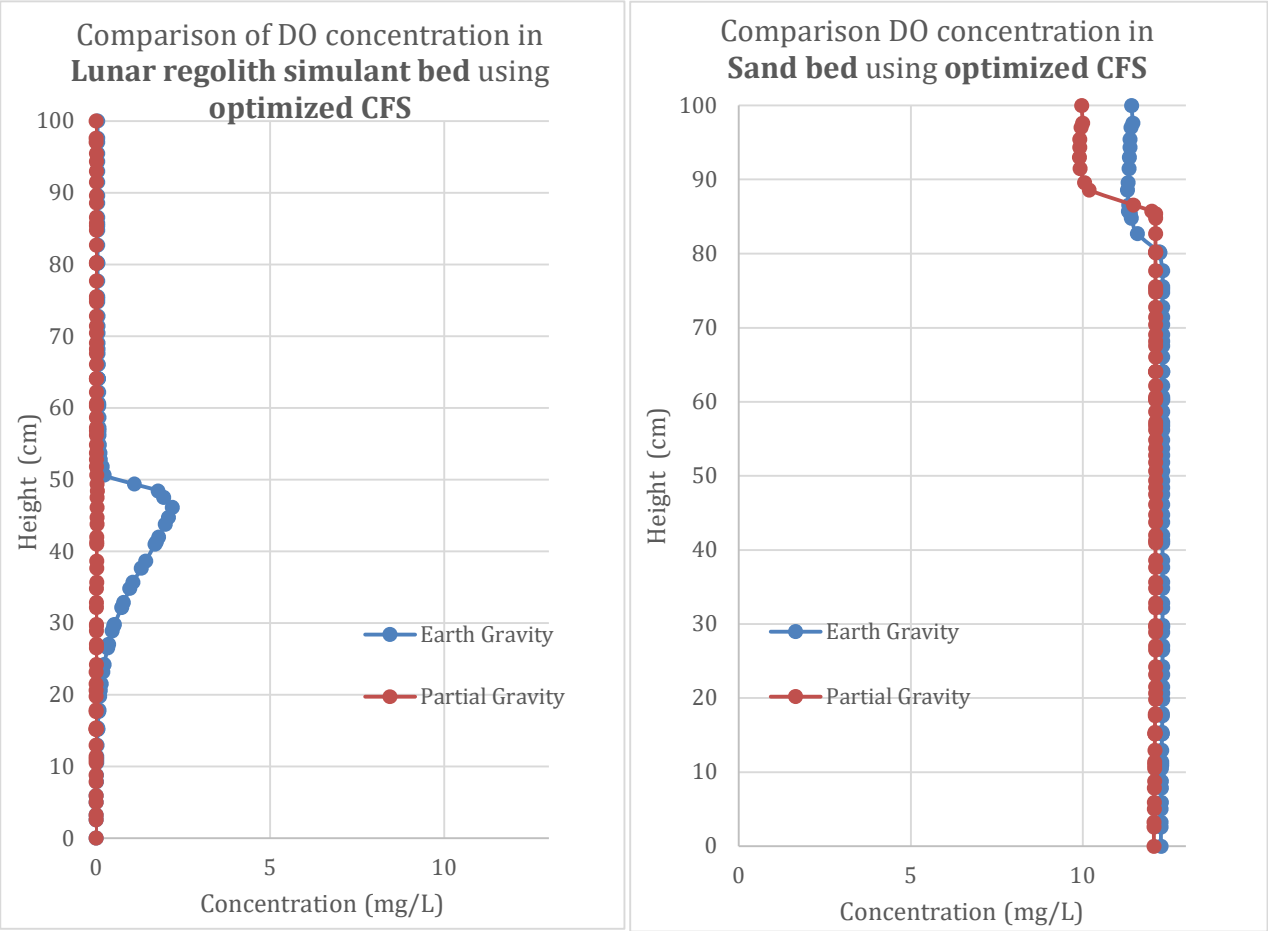

Figure: 4.2.2(a),(b).: Figure shows the dissolved oxygen (DO) concentration in two substrate bed (lunar regolith simulant (LMS-1) (a) (left) and sand (b) (right) at the 30th day throughout the bed height using optimized CFS

The higher reduction in rCOD and sCOD in sand in CFS could be attributed to the higher cohesion in sand compared to lunar regolith simulant, the cohesion of sand is 11.17 kPa compared to 0.393 kPa for lunar regolith simulant (specifically LMS-1) which is almost 30 times higher. This property is an advantage for reduction in rCOD and sCOD. Higher cohesion allows the substrate enough contact with the microorganisms and more contact area for microbial and physicochemical conversion. This could be the be seen seen by higher values of iCOD in the case of sand (532.9 mg/L) compared to lunar regolith simulant (203.9 mg/L) in earth gravity.

Another limiting factor in contaminant removal is the concentration of dissolved oxygen (DO) in the bed, which starts out higher in an empty porous bed of substrate due to pores being filled with air while the surface is exposed to the atmosphere as shown in Figure 4.2.4. (a), (b). Initially a considerably higher concentration of DO (9 mg/L) can be observed start of the simulation for both substrates. This initial high concentration reduces upon addition of wastewater having a DO concentration of 0.282 mg/L for lunar regolith simulant but increases over time of the bed in sand as shown in Figure 4.2.4 (b) at saturated conditions (30th day). (a) shows a very low DO concentration in lunar regolith simulant and almost zero oxygen permeation in partial gravity (0-0.03 mg/L). Compared to sand which allows for easy permeation of oxygen over the bed even in partial gravity (b).

The DO in sand bed increases overtime from 9 mg/L to 12 mg/L and remains constant over the depth of the bed. This shows that the wetland aeration is indeed affected by parameters like depth and size of gravel[78]. If this result could be attributed to the difference in the nature of lunar regolith simulant and sand, a possible hypothesis is that sand pores allow for easier absorption of oxygen from the empty pores. However, lunar regolith simulant does not allow for easier exchange between the gas-liquid. This is further discussed in Section 5.2.

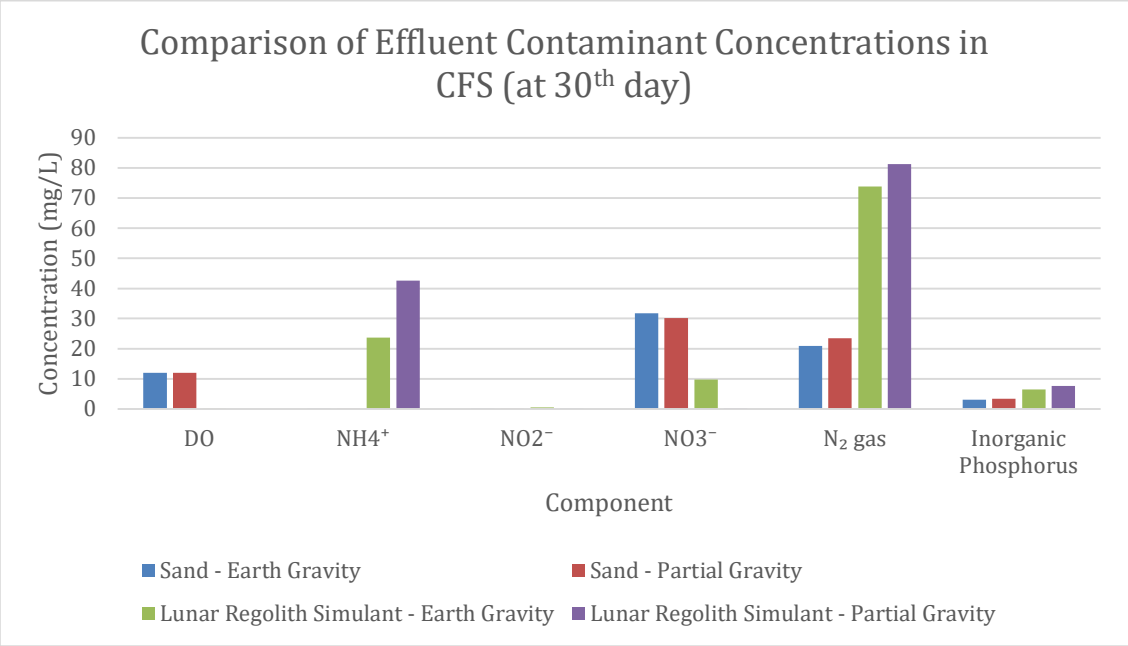

Figure 4.2.3: Figure shows the simulation results from HYDRUS-2D for comparison of effluent concentrations simulated for different compoenents in wastewater at 30th day of treatment using CFS.

DO is interlinked to microbial processes, specifically for processes that are dominant in rCOD removal like aerobic degradation, respiration by heterotrophs and nitrification. Therefore the rCOD removal throughout the bed depends on the DO available[59]. In HYDRUS CW2D module, sCOD does not use DO

for conversion into rCOD for hydrolysis (see Section S1). It can therefore be observed in Figure A4 (Annex), sCOD decreases but the increasing rCOD is not degraded due to the lower DO concentration previously shown in Figure 4.2.2 (a).

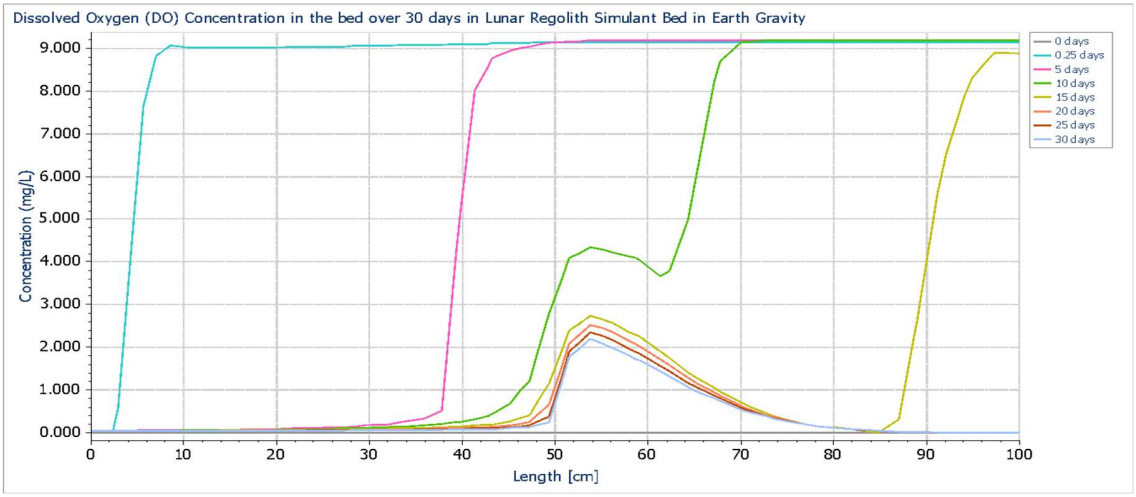

(a)

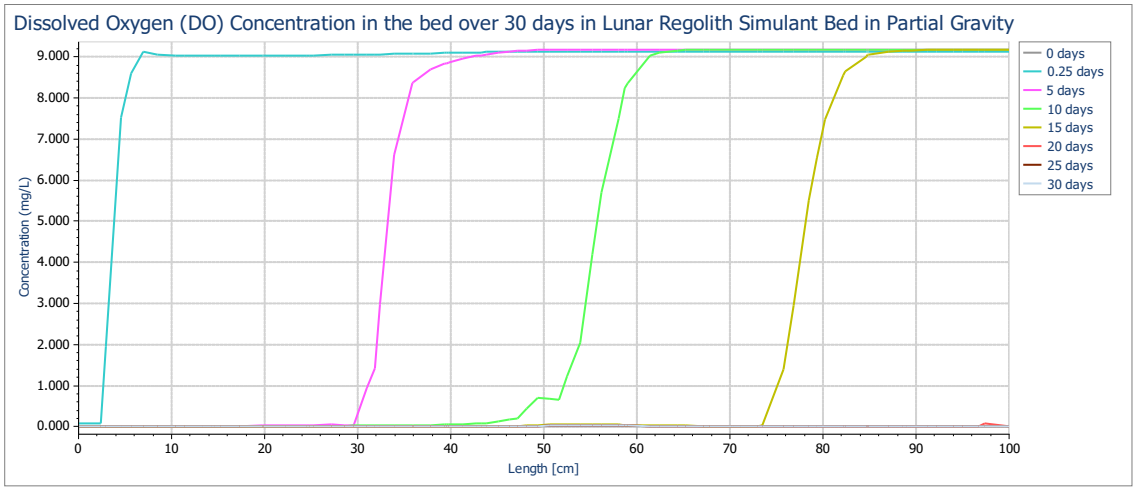

(b)

Figure 4.2.4: Figure shows concentration of DO throughout the bed depth (0 cm being the surface) at different time points through 30 days using CFS for lunar regolith simulant in earth (a) and partial gravity (b)

The effect of DO also evident in the nitrification process. A threshold of 1.5 mg/L required for nitration process[79]. Since there is higher DO in earth gravity at steady state conditions. Nitration process could perform better in earth gravity which aligns with the fact that higher amount of NO_3^+ (9.7 mg/L) are shown in simulation results in this condition as shown in Figure 4.2.3.

Further due to these anaerobic conditions, more ammonium (NH_4^+) in lunar regolith simulant bed could be converted to dinitrogen gas (N_2) via the anoxic process modelled in HYDRUS. This is inline with the increased N_2 content using lunar regolith simulant in partial gravity (81.27 mg/L) and earth gravity (73.76 mg/L). On the other hand, since sand has been shown previously to provide good aeration and DO concentration throughout the bed at saturation, aligns with the fact that more of the NH_4^+ has convert into nitrates (~30 mg/L) and dinitrogen gas (~20 mg/L) for both earth and partial gravity in sand substrate (see Figure Figure 4.2.3).

The optimized CFS does not provide satisfactory COD removal in the effluent with lunar regolith simulant (52.5% total COD removal in earth gravity and 14.9% in partial gravity) is still considerably high and not treated enough according to EU Urban Waste Water Treatment Directive 91/271/EEC[80], which requires treatment of urban wastewater to a total COD of 125 mg/L or a reduction in COD of 75%. Other feeding strategies are explored in the next section to check the nutrient removal specifically using lunar regolith simulant. Furthermore, since NO_3^- is an important nutrient for plant growth, aerobic conditions are important to be maintained in the partial gravity system and these conditions can be further enhanced by modifying the design to increase the aeration. Furthermore, the size of the gravel/substrate bed used is also related to oxygen transfer efficiency[78].

Since the design of the plant is to optimize for autonomy and reduced intervention, using an operation strategy which allows natural aeration into the bed or more time for the solute to be processed in the bed is required. This provided a considerable insight from the initial results of contaminant removal in optimized CFS and a basis for investigating contaminant removal in an IFS strategy.

4.2.2. Simulation results of nutrient removal using IFS

The IFS strategy is providing enough downtime to allow the wastewater contaminants to be processed by the microbial activity. As we observed from the previous simulation results that the optimized CFS for 40 L/day wastewater feeding directly to the bed was not effective in COD removal and removed only 15% of total COD in lunar regolith simulant in partial gravity. This was attributed factors such as DO and inherent substrate properties. Since these properties of lunar regolith can not be changed, a viable strategy is to change the current operation/feeding again to allow more time for biological transformations specifically aerobic transformations by oxygen permeation for contaminant removal. Such a strategy implemented is IFS strategy, whereby 40 L of wastewater is added to the bed and it is provided downtime of 10 days. Table 4.2.5 shows the results of simulation of contaminant removal using IFS for operation of the system whereby the wetland bed is fed with 40 L of wastewater once every 10 days in lunar and earth gravity. This feeding strategy was selected after several trials by increasing downtime (from 1 day to 10 days), therefore increasing the downtime of the system to 10 days was the optimized IFS.

Table 4.2.5: Table shows the simulation results from HYDRUS-2D for 60th day using sand and lunar regolith simulant bed with IFS (10 day intervals and addition of 40 L of wastwater) in partial and earth gravity

Component	**Gravity**	**Substrate**			
		Sand		Lunar regolith simulant (LMS-1)	
		Earth	Lunar	Earth	Lunar
	Influent	Effluent			
Readily biodegradable COD (mg/L)	1600	3.35	0.99	75.94	3.82
Slowly biodegradable COD (mg/L)	1200	5.43	3.75	55.33	6.23
Inert COD (mg/L)	200	604.96	605.85	254.91	122.07
Ammonium ion (NH_4^+) (mg/L)	50	0.01	0.01	0	0
Nitrite ion (NO_2^-) (mg/L)	3	0	0.002	0.02	0.03
Nitrate ion (NO_3^-) (mg/L)	30	109.03	105.69	0.17	0.61
Dinitrogen gas (N_2) (mg/L)	0	34.38	44.08	108.14	53.49
Phosphorus (inorganic) (mg/L)	116	29.19	30.5	3.34	1.69

As shown in Table 4.2.5, compared to the previously tested optimized CFS summarized in Table 4.2.1, the effluent concentrations are drastically different for the total COD removal (%) in lunar regolith simulant. From 52.5% to 86.15% in earth gravity and 14.9% to 95.9% in partial gravity, showing that contaminant removal processes could be occurring more effectively in this strategy. Furthermore, the contaminant removal is higher in lunar regolith simulant in lunar gravity compared to earth gravity for COD removal showing the efficacy of this strategy. However, the nitrate (NO^{-3}) concentrations are reduced to almost negligible (0.17-0.61 mg/L) using lunar regolith simulant showing high removal of nitrates (98-99%). The effluent still contains a minimal concentration (~1-3 mg/L) of inorganic phosphorus.

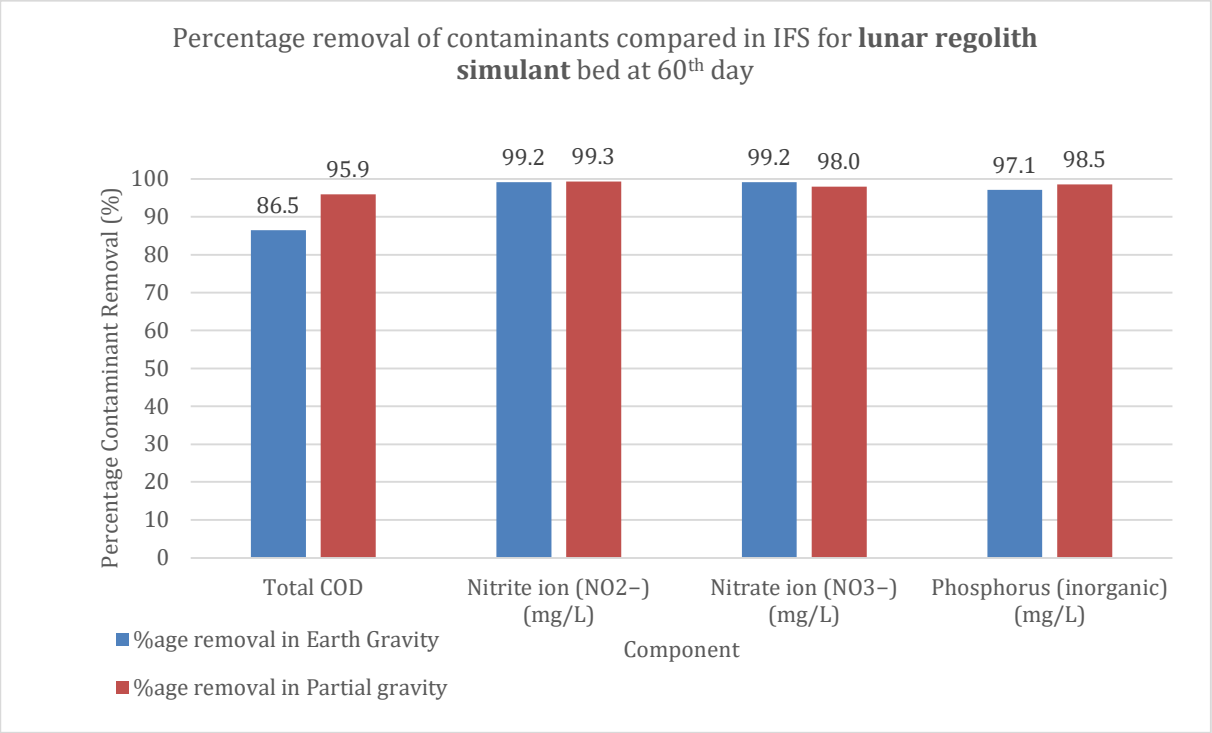

Figure 4.2.6: Figure shows the percentage removal (%) calculated from HYDRUS-2D results for specific contaminants achieved by using IFS with a downtime of 10 days, in earth and partial gravity

To understand the difference in the activity and mechanism behind the higher contaminant removal rate with increased downtime, it is important to investigate the important parameters over time in bed and how they behave differently. One of the most important parameters discussed in the last section is the DO content over the bed as it drives not only the COD removal but also the nitrogen transformations. It can be observed from Figure 4.2.7 (b) below that the lunar regolith simulant bed remains partially air saturated upon feeding only once in ten days, and over time allows enough oxygen in the lower portion (50-100 cm) of the bed for

effective transformation of rCOD. This could be attributed to aerobic degradation in the bed that led to COD removal. In this strategy the dissolved oxygen (DO) adaptation is similar to the sand bed.

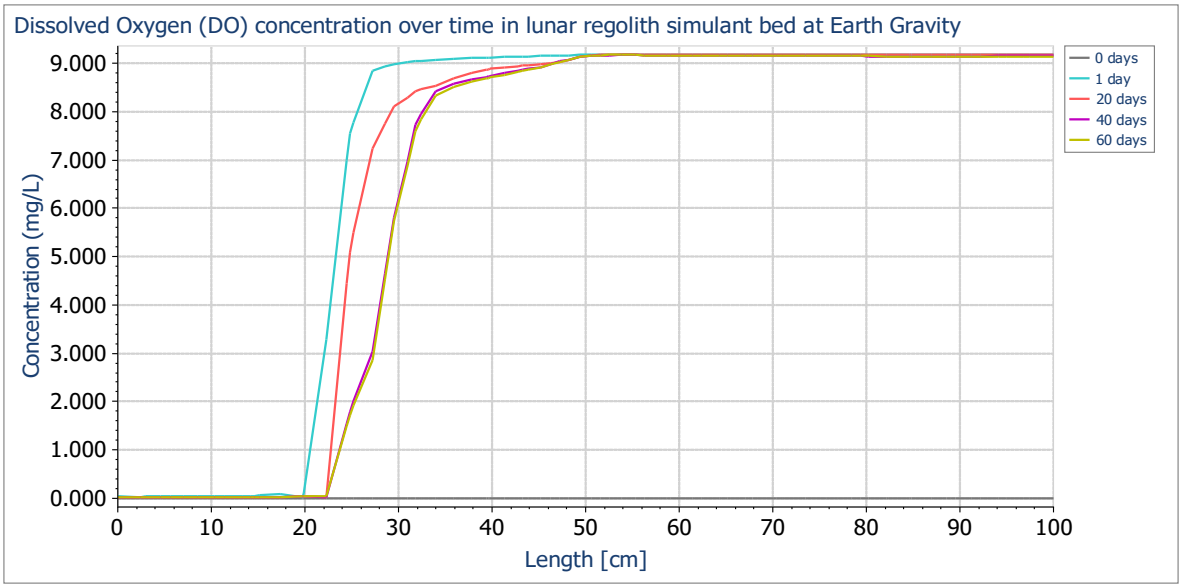

(a)

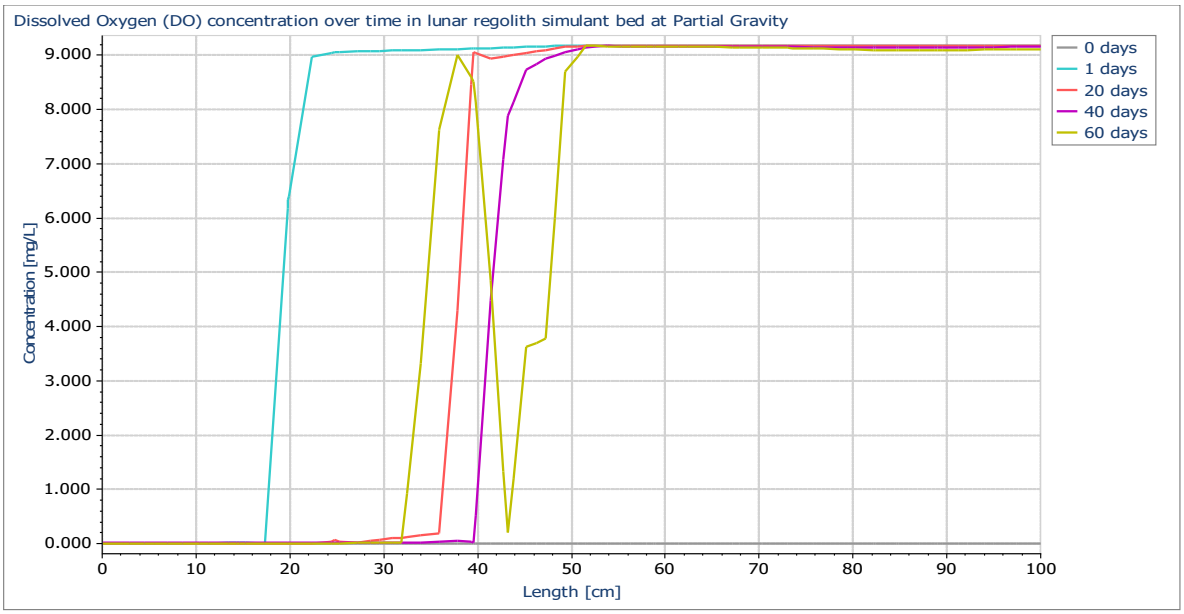

(b)

Figure 4.2.7: Figure shows the concentration of DO throughout the bed depth (0 cm being the tallest point) at different points through 60 days using IFS 540 L every 10 days) for lunar regolith simulant in earth (a) and partial gravity (b), results taken directly from HYDRUS-2D

It can be observed from Figure 4.2.8 (a), (b) that the DO profile over time is relatively different from the optimized CFS DO profile shown in Figure 4.2.2. This is shown by the increased fluctuation of DO around 20 cm of bed. Since the time points show the profile at the day of feeding, the DO reaches a certain height at day of feeding. Further the bed allows for an exchange between the DO from the atmosphere once all of the wastewater has passed through the bed. This can cause further increase in the dissolution of oxygen for continuing microbial processes. It can also be observed from Figure 4.2.8 (a), (b) that DO is also affected by the lower gravity in the partial gravity regime, allowing for more penetration of the DO through the bed at 60th day in partial gravity.

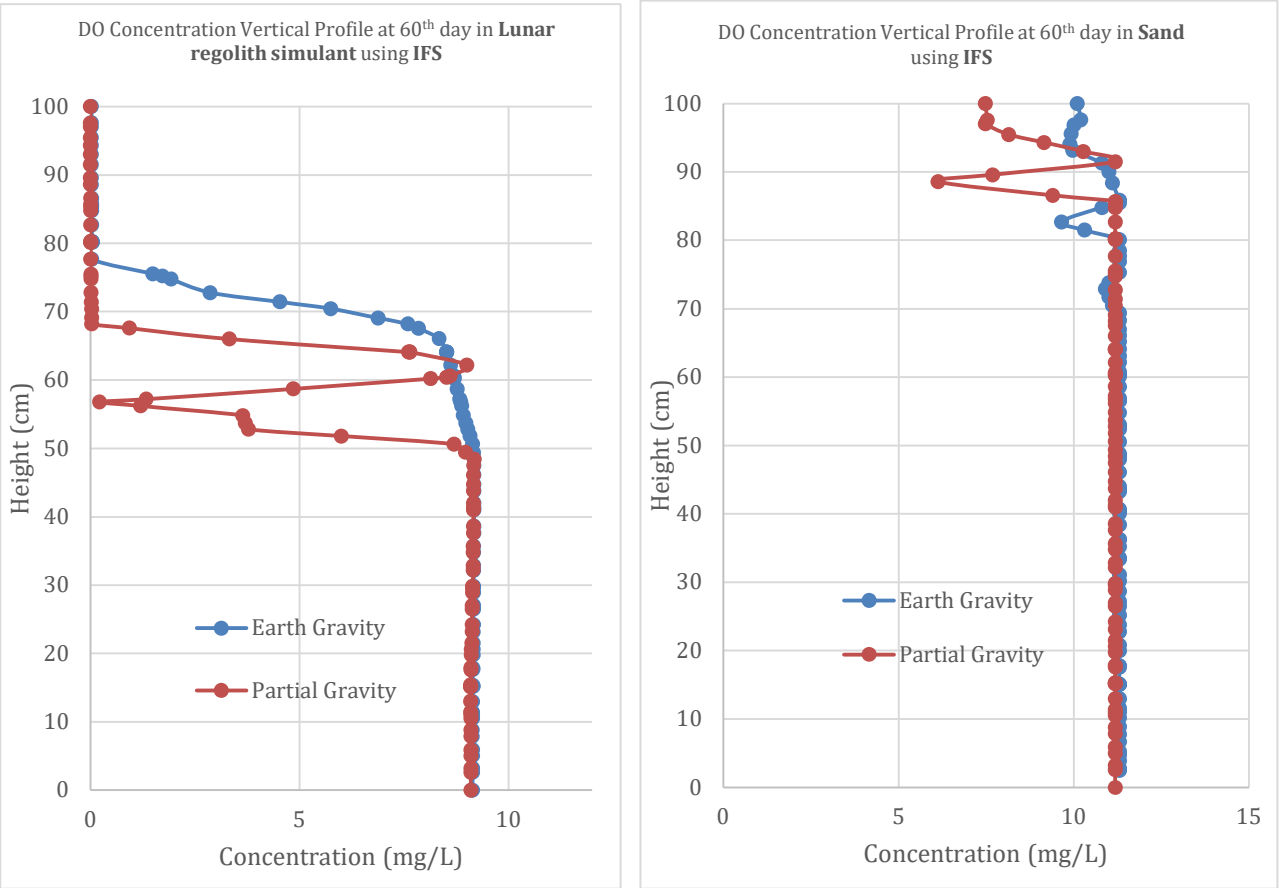

Figure 4.2.8 (a), (b): Figure shows the simulation results from HYDRUS-2D for DO profile through the bed at 60th day in both gravity regimes for lunar regolith simulant bed (left) (a) and sand (right) (b)

Comparing the results in Figure 4.2.7 to previous DO profile in Figure 4.2.4 using optimized CFS. The results are similar in the start of the bed due to the structural difference and higher oxygen-to-water transfer supporting this hypothesis from Section 4.2.1. For lunar regolith simulant in partial gravity, to obtain sufficient COD removal, one of the limiting factors in this case is the time required for slower

oxygen-water transfer required for aerobic degradation of rCOD. The organic matter and other solutes pass through the bed at a slower rate than wastewater. Therefore, the bed accumulates contaminants like COD overtime. Due to limited DO, the COD cycle starts but is not completed causing an increased rCOD. This rCOD as dissolved organic matter passes through the bed with water lower intervals (5, 7 days) using lunar regolith simulant.

The effluent COD distributions over time for 60-day simulations using intermittent strategy are shown in Figure 4.2.9 (a) for earth gravity and Figure 4.2.9 (b). It can be observed that this strategy allows for enough time for the bed to remove the rCOD despite limited DO so that the effluent contains little to no rCOD and sCOD (also shown in the concentration profiles in Figure A3 (Annex)). The effluent still contains considerable amount of inert COD (sludge) which cannot be removed through the bed due to biological transformations, and these contribute mainly to the COD left in the effluent, this could be due to the lysis process mentioend in S1 (Supporting Information).

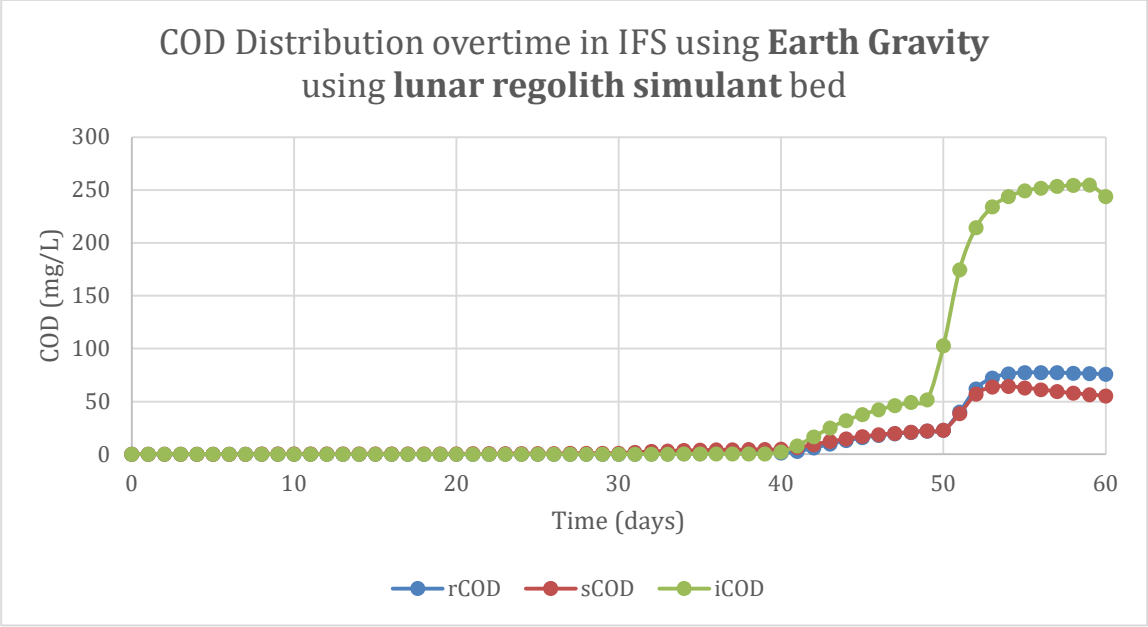

Figure 4.2.9(a): Figure shows the simulation results from HYDRUS-2D for change in effluent final COD distribution over time in earth gravity from lunar regolith simulant bed for 60-day simulation

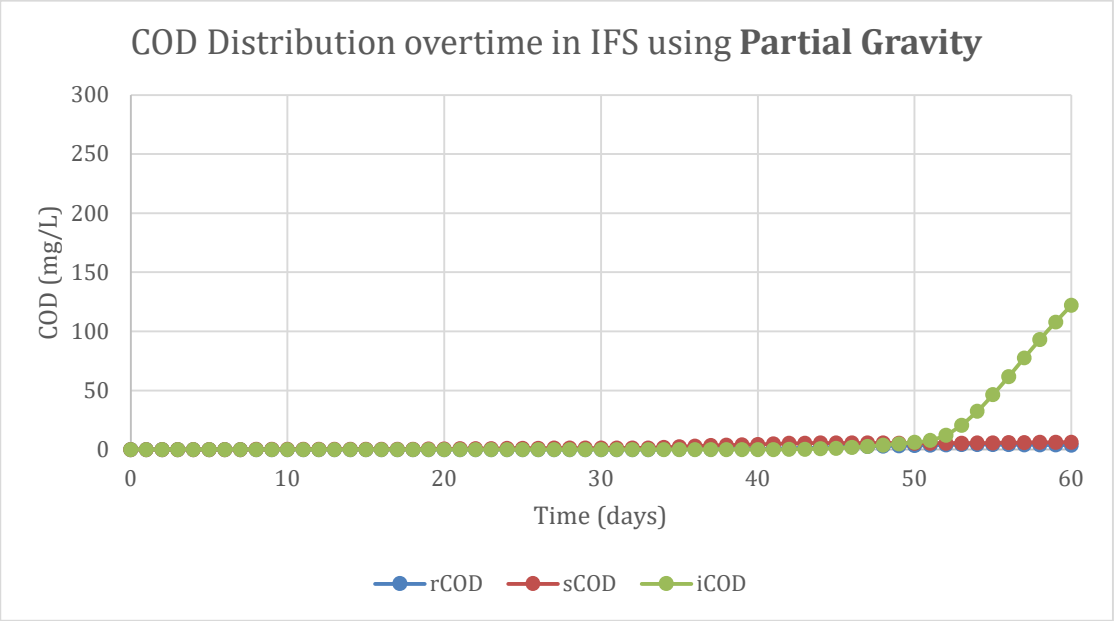

Figure 4.2.9(b): Figure shows the simulation results from HYDRUS-2D for change in effluent final COD distribution over time in partial gravity from lunar regolith simulant bed for 60-day simulation

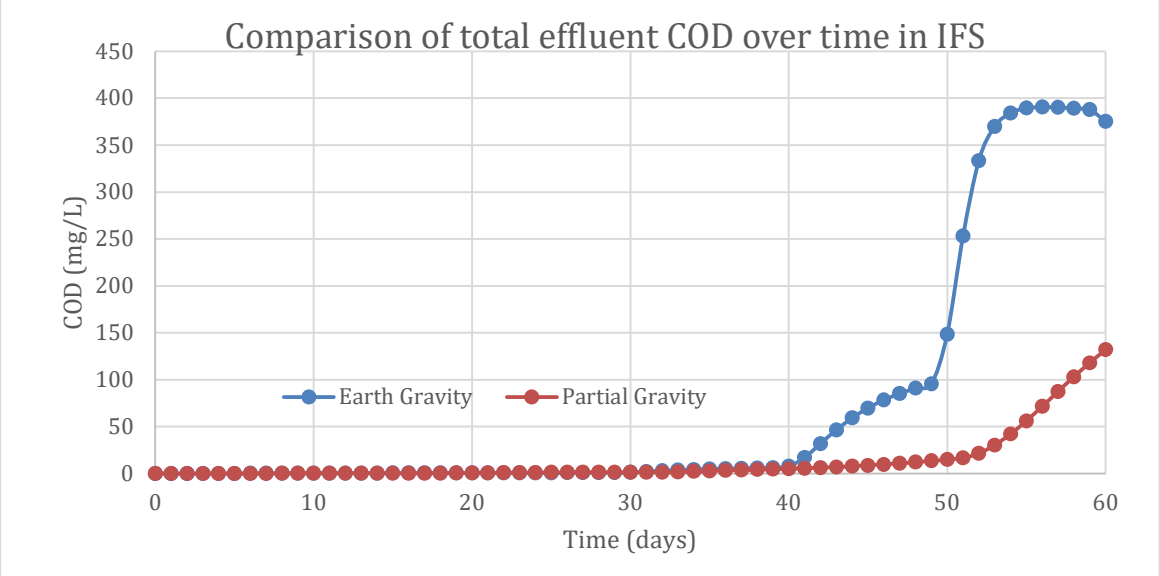

Figure 4.2.10: Figure shows the simulation results from HYDRUS-2D for comparison of effluent total COD comparison in earth and partial gravity from lunar regolith simulant bed for 60-day simulation using IFS

Fom Figure 4.2.10, it can be observed that the COD removal in intermittent strategy is higher in partial gravity compared to earth gravity. This is due to less accumulation of inert COD in partial gravity potentially because of lower cell lysis and due to a better DO profile. It can be observed in Table 4.2.5 and

in Figure A3, that the dinitrogen content obtained using lunar regolith simulant is considerably higher than in sand, owing to lack of DO and could be due to the anoxic transformations occurring at the end of the bed.

Chapter 5: Discussion

5.1. Substrate properties

Simulation results of hydrodynamic comparison of lunar regolith simulant and sand show that sand shows a higher water permeability (0 L/day accumulation at saturated condition) compared to lunar regolith simulant. This in accordance with Tabuchi et al., 2023 which states that water permeability of lunar highland regolith simulant (LHS-1) is 1-2 orders of magnitude lower than fine silica sands at similar packing fractions, attributed to irregular particle shapes and micro-sized chunks[81]. Although the simulant (LMS-1) properties used in the hydrodynamic simulation due to the geo-location difference in regolith type (refer to Figure A1, Annex), this result still holds true. The difference between the permeabilities of sand and LMS-1 could not be verified distinctively through simulation results, even though the water blocking properties of regolith pointed out by Chevrier et al., 2006[82] manifested as shown in Section 4.1.1.

It can be pointed out that the saturated hydraulic conductivity in earth gravity of LMS-1, empirically measured by Brozovich et al., 2024[54], are similar to the estimated value using Karman-Cozeney correlation for LHS-1, 15-19 cm/day and 13.24 cm/day respectively. LHS-1 shows a slightly lower saturated hydraulic conductivity even though both have a considerable difference in mineralogical composition [83]. This allows for more flexibility between using different types of simulants for validating the simulation results as it hints that the geographic location of lunar regolith might not affect the hydrodynamic properties of the regolith to a larger extent.

However, this similarity in the saturated hydraulic conductivity could also be because of the same manufacturing company of the simulants (Exolith labs). Therefore, it is important to characterize the hydraulic parameters of other mare and highland simulants from other manufacturers such as LX-M100 (mare simulant to be characterized for validation of simulation results and prototyping phase). Furthermore, upon initial investigation of the hydraulic conductivity of lunar regolith simulant (LX-M100) done in the context of this project, a bigger particle size range (1-2 mm) for checking for countering reduced gravity effects is envisioned as increasing particle diameter above 1 mm and narrowing particle size distribution may be beneficial[84].

Sand has rounder grains, less dust particles and the saturated hydraulic conductivity (K_{sat}) of sand is almost 43 times higher compared to the saturated hydraulic conductivity (K_{sat}) of lunar regolith simulant (see Section 3.4). The difference in saturated hydraulic conductivities (K_{sat}) does not only manifest in the

movement of water through the bed but also in solute transport by affecting the contaminant removal mechanisms like advection and dispersion. Higher hydraulic conductivity (K) allows for greater longitudinal dispersion as shown Section 3.4, causing solute plumes to spread out more in sand in shorter time compared to lunar regolith[85]. This property of sand is different from the natural water blocking property of regoliths[82] which manifests as higher transverse dispersibility in lunar regolith.

Another important factor is the inherent difference in the solute transport properties of lunar regolith and sand as shown in Table 3.4.2, where lunar regolith has a higher transverse dispersibility (1.96 cm) while sand has a higher longitudinal dispersibility (0.5 cm). This makes sand a better candidate for use in VFCW and lunar regolith as a better candidate for use in horizontal flow vertical flow wetland (HFCW). Furthermore, properties of lunar regolith show a lower accumulation of sludge (inert COD) as shown in the result of nutrient removal, lower sludge accumulation in lunar regolith simulant aligns with findings that less cohesive, finer-grained substrates produce less long-term clogging but may compromise treatment efficiency[76].

It should be considered that a big limitation while discussing the HYDRUS simulation results is not taking into account the heterogeneity of the hydraulic conductivity and non-uniform surface distribution of the water which can lead to further reductions in filtration depending on the properties of the substrate [85]. Over time, the effect of organic matter added on hydraulic conductivity is also not simulated and can be different for each substrate leading to specific clogging issues. The addition of organic matter increases substrate fertility however, higher amounts of organic matter might reduce the hydraulic conductivity further [86].

5.2. Dissolved oxygen (DO)

The importance of DO for nitrification and overall treatment efficiency is well-established in wetland and biofilter literature [85]. The DO concentration throughout substrate bed is shown to be affected by the substrate properties in both optimized hydrodynamic and intermittent feeding strategies. Sand shows better DO permeability in both cases. The result is consistent with the simulation parameter α (inverse of air entry suction pressure). α for sand (0.145 m^{-1}) and lunar regolith simulant (assumed as 0.02 m^{-1}) was used in the simulation as shown in Table 3.4.1. α is higher for sand than in lunar regolith simulant which means that sand requires less suction pressure for air to enter the pores than lunar regolith simulant. This could be the reason why the oxygen is not properly when incoming wastewater is added on the bed in lunar regolith simulant, therefore the oxygen is pushed down with added water over time, as shown by the results in Section 4.2.1.

It is important to mention that this α was based on assumption of properties of hydraulic properties of lunar regolith being similar to silty loam as shown by Brozovich et al., 2024[54] and mentioned in Table

3.4.1. Therefore, to critically discuss the sensitivity of the intermittent feeding downtime to this parameter, sensitivity analysis was conducted in partial gravity for lunar regolith simulant. It was observed that with increasing value of α, the intermittent feeding time was reduced to 9 days for and increase in air entry suction pressure from 0.02 m^{-1} to 0.05 m^{-1}. Even though this result provides an insight that the substrates with higher air-entry suction pressure could further reduce the solute transport by decreasing the time required for oxygen permeation. Future research should be focused on empirical measurement of this parameter for lunar regolith simulant to obtain better understanding of the DO mechanism in lunar regolith. α can be changed by various soil properties, including mineral composition, swelling properties, and grain size distribution[87]. Therefore, manipulation of these properties could provide a different result in terms of DO exchange in the porous bed.

A factor to consider while interpreting the HYDRUS results of DO like other solutes simulated is that they are dissolved in wastewater. The initial bed is in dry condition but still contains some amount of moisture at field capacity. It should also have a higher linked DO content which was not added in the initial conditions. The importance in substrate's ability to transfer DO is the main effect manifested in the difference between two substrates simulated. Based on this observation, the properties oxygen-transfer properties of both sand and lunar regolith simulant have been compared.

5.3. Effect of gravity

The main differences in partial and earth gravity manifests as the reduced infiltration and accumulation on top of the bed which is not observed in both substrates at earth gravity. Further lunar regolith simulant bed takes longer time to achieve saturation (6 days) compared to earth gravity (4 days). This simulation result was in accordance with the fact that particle size and gravity levels can influence infiltration rates[45]. The phenomena of reduced speed of infiltration in lower gravity observed in Section 4.1 was expected to allow for higher contamianant removal in partial gravity. However the contaminant removal performance of the two substrates (sand and lunar regolith simulant) did not present considerable difference for total COD removal (%) in optimized hydrodynamic strategy in the two gravity conditions tested due to difference in substrate properties. Therefore, it is more relevant to compare the effect of gravity on the same substrate rather than comparing substrates to one another.

Even though sand behaves slightly better in earth gravity (0.6%), this difference is not very significant and shows that the hydraulic properties of the substrate like cohesiveness and solute-transport properties are more important than the gravity conditions for substrates with high saturated hydraulic conductivity like sand (712.8 cm/day). This could also suggest that gravity-dependent effects on water movement in porous media may be limited to specific conditions, such as large particle sizes or high porosity allowing particle movement[88].

The water-blocking effect of lunar regolith[82] was more pronounced in partial gravity shown in Section 4.1 and required modification of the loading technique. However it did not show the threshold contaminant removal (>75%) using optimized CFS (Section 4.2.1). Therefore, the crucial factor where gravity condition can play a big role is determining a hydrodynamic strategy which does not cause accumulation and reduction in infiltration rate while still producing acceptable contamiannt removal. However it can be observed by the results of IFS (Section 4.2.2) that partial gravity favored the removal of rCOD and sCOD showing (+95% removal) while not retaining much of the iCOD due to lower cell lysis. This could be a potential benefit of using partial gravity, however the increased downtime required for contaminant removal (10 days) is a significant disadvantage since similar contaminant reductions can be achieved for lower downtime in earth gravity using lunar regolith simulant.

5.4. Feeding strategy

Lower hydraulic conductivity of lunar regolith allows the solute to move slowly through the bed as the water passes slowly through the substrate. This increases time especially at the top of the bed, potential for reactions and attenuation of the solute. This inherent difference in hydraulic properties could explain higher removal of organic matter (COD) for sand when more of the wastewater is added in a short time, 8 hours (optimized CFS) and better performance of lunar regolith simulant when wastewater is added at once and the bed is left for processing for longer residence times, 10 days (IFS). Furthermore, better performance of sand in optimized hydrodynamic strategy shows that the bed could be reduced in size to achieve a permissble range of COD removal (%). The main culprit for incomplete COD removal in optimized CFS was poor aeration conditions which were successfully verified by the simulation results in Section 4.2.1.

The difference in the DO profiles in the two feeding strategies is in further accordance with Wanko et al., 2006[89], which shows that the dominant oxygen transfer mechanism in porous bed is convection in continuous feeding, while diffusion plays a minimal role in deeper layers. This could be the case in lunar regolith where this is lack of convection and the dominant oxygen transfer is occurring by diffusion owing to reduced hydraulic conductivity and longitudinal transversality.

The optimized CFS in partial gravity using a lunar regolith bed has a high saturation time of 14 days, this can be a disadvantage as it requires more time for the set-up of the system. Using a slightly different feeding schedule, the saturation time can be decreased for allowable accumulation on top of the bed if the design of the VFCW allows it. Recent studies have explored innovative designs, including constructed floating wetlands (CFWs) that adapt to changing water levels[90] and hybrid systems combining vertical and horizontal flow[17]. However, using such a system requires more complex machinery than a passive design approach required in the scope of this research.

Feeding strategies can be modified based on the priority whether the system prioritizes more water passing through the bed (CFS) with a compromise on effluent quality or whether the system prioritizes effluent quality and compromises on time (IFS). However, the two strategies can be used with design modifications such as introducing aeration techniques and allowing for higher residence times in the bed [91]. Another approach is effluent recycling back to the VFCW bed[92], however this requires introduction of pumping machinery.

5.5. Nitrification rates

One of the disadvantages of the IFS is that it allowed conditions for the nitrogen cycle to pass through directly from ammonium (NH_4^+) to dinitrogen gas (N_2) and competition between aerobic degradation and nitrification due to lower DO[91]. Since the aim of the study is to enhance nitrate, this can manifest as a disadvantage and further design modifications need to be added such as aerations at the bottom of the bed. There is more concentration of nitrates (NO^{-3}) in the effluent using sand-substrate compared to lunar regolith simulant because of better availability of DO. The results show that there is indeed a competition between the aerobic degradation and nitrification process as the nitrate concentration using lunar regolith simulant in both gravity conditions is almost 0 mg/L as mentioned in Liu et al., 2016 for the case of lunar regolith simulant. However, minimum nitrogen concentrations for maximum growth can be as low as 2-20 mg/L for some crops[93]. Therefore, future strategies should optimize the substrate performance for achieving higher nitrate concentrations in the effluent for the effluent to be used for potential agricultural and hydroponic utilization.

Chapter 6: Conclusion & Recommendations

6.1. Conclusion

This study evaluated the feasibility of CWs beds using lunar regolith simulant and sand for BLSS under Earth and partial gravity. Results showed that substrate properties, especially hydraulic conductivity and particle structure, are critical for water movement, contaminant removal, and oxygen transfer. Sand, with its higher hydraulic conductivity, enabled faster infiltration and more stable saturation, while lunar regolith simulant's lower permeability led to slower infiltration and greater surface accumulation, particularly under partial gravity. Contaminant removal depended on both substrate and feeding strategy. With optimized CFS (12 L every 7–8 hours), sand achieved high COD removal (~81.9%), but lunar regolith simulant performed poorly in partial gravity (14.9%) due to limited hydraulic conductivity and poor oxygen transfer. Dissolved oxygen availability was a key limiting factor, as the regolith simulant showed near-zero DO at saturation, inhibiting aerobic degradation. Switching to an IFS (40 L every 10 days) greatly improved COD removal in lunar regolith simulant (up to 95.9% in partial gravity), but this also led to prolonged anoxic conditions,

favoring denitrification and causing significant nitrate loss. Sand maintained better nitrate recovery due to more consistent oxygen distribution. These findings highlight the trade-off between contaminant removal and nutrient recovery, emphasizing the need for careful selection of substrates and feeding strategies. In summary, while lunar regolith simulant can be adapted for effective organic contaminant removal in partial gravity with optimized intermittent feeding, its limitations in oxygen transfer and nitrogen cycling pose challenges for nutrient recovery. Future designs should focus on aeration techniques recommended to meet the COD removal effectively, while using CFS to manage the required load (40L/day).

6.2. Recommendations

Based on the results of simulation, discussion and conclusion, the recommendations for design and operation of VFCW in the context of this study are summarized in Table 6.2.1 and Table 6.2.2.

Table 6.2.1: Table shows the design recommendations for the system based on simulation results

Design Area	Recommendation	Expected Benefit
Substrate Engineering	Improve lunar regolith simulant with a higher particle size of 1 mm, optimize for mineral composition, swelling properties, and grain size distribution for increase air suction into bed pores	Enhances infiltration, reduces surface accumulation, supports stratified biological activity.
Bed Geometry	Design beds to be shallow (≤80 cm) and wide, with gentle slopes. Use modular rectangular units if needed.	Improves oxygen penetration and uniform saturation; better hydraulic performance under reduced gravity. Boosts Nitrate (NO_3^-) formation
Aeration Enhancement	Incorporate passive aerators (e.g., perforated tubing) in lower layers. Consider surface air exposure vents.	Improves DO availability, supports aerobic microbial processes, essential for COD and nitrate removal. Boosts nitrate (NO_3^-) formation
Flow Distribution System	Use perforated inlet manifolds or drip feeders to distribute uniformly across the bed surface.	Prevents channeling, ensures equal treatment across the bed, avoids dead zones.
Monitoring & Sensor Integration	Install embedded sensors for DO, NH_4^+, NO_3^-, temperature, and moisture at various depths. Connect to data logging and control systems.	Enables real-time monitoring and adaptive system control, especially in autonomous or remote setups.
Modular Design	Use tray-based or cartridge-style replaceable substrate compartments. Include accessible ports for inspection and replacement. Include a retention compartment for receiving treated water at the end	Simplifies maintenance, especially important for long-term closed-loop systems (e.g., lunar bases), allows better control of the treated effluent

Table 6.2: Table shows the operational recommendations for the system based on simulation results

Operational Focus	Recommendation	Expected Benefit
Feeding Strategy – Intermittent	Use IFS with shorter intervals via automated valves with programmable timers.	Allows oxygen recovery between cycles; significantly improves COD removal (up to 95.9% in partial gravity).
Feeding Strategy – Distributed Daily Load	If daily treatment is required, split load into multiple alternating VFCWs	Allows higher quantity of water to be treated based on the size of the crew
Nutrient Recovery Enhancement	Promote aerobic stage or air-permeable zone near bed bottom to favor nitrification over denitrification.	Promotes nitrate formation, reduces conversion to dinitrogen gas, aiding plant nutrient recovery.
Automated Control System	Employ programmable logic controllers (PLCs) or microcontrollers to manage inflow, aeration, and sensor feedback for level control	Improves system autonomy, essential for space missions or minimally supervised environments.
Innoculation and Microbial Processes	Follow a proper start-technique and cultivation of microbiota by using terrestrial wastewater as an influent	Enhances long-term biological performance, prevents rapid decline in hydraulic conductivity.
Energy Optimization	Use gravity-fed inflow where possible and solar-powered components for electronic load.	Reduces energy requirements, supports sustainability and closed-loop design for space-based systems.

Based on the following recommendations, figure 6.1 shows the implemented changes for design and operational scheme in the initial conceptual model of 'the Marshian' system.

6.3. Future directions

Future research will focus on experimentally determining the hydraulic properties of the lunar mare simulant (LX-M100) under Earth gravity to validate the hydrodynamic simulation results. Additionally, a highly-concentrated wastewater with total COD concentrations ranging from 3000 to 4000 mg/L will be formulated for use in prototype testing. These experimental data will support the refinement of influent parameters used in the simulation model.

Subsequent simulation efforts should aim to further optimize the operational strategy of the vertical flow constructed wetland for long-term wastewater management in a four-astronaut lunar base scenario. Particular attention should be given to enhancing the removal of nitrate (NO_3^-) and phosphorus (P), which may benefit from incorporating vegetation into the system. The effect of planting on contaminant removal dynamics particularly nutrient uptake, microbial enhancement, and oxygen transfer should be explored.

To improve model calibration and accuracy, tracer experiments may be conducted in future work to validate solute transport behavior and refine initial condition assumptions. These efforts will support the development of a reliable, compact, and bioregenerative treatment system suitable for both extraterrestrial and land-constrained terrestrial applications.

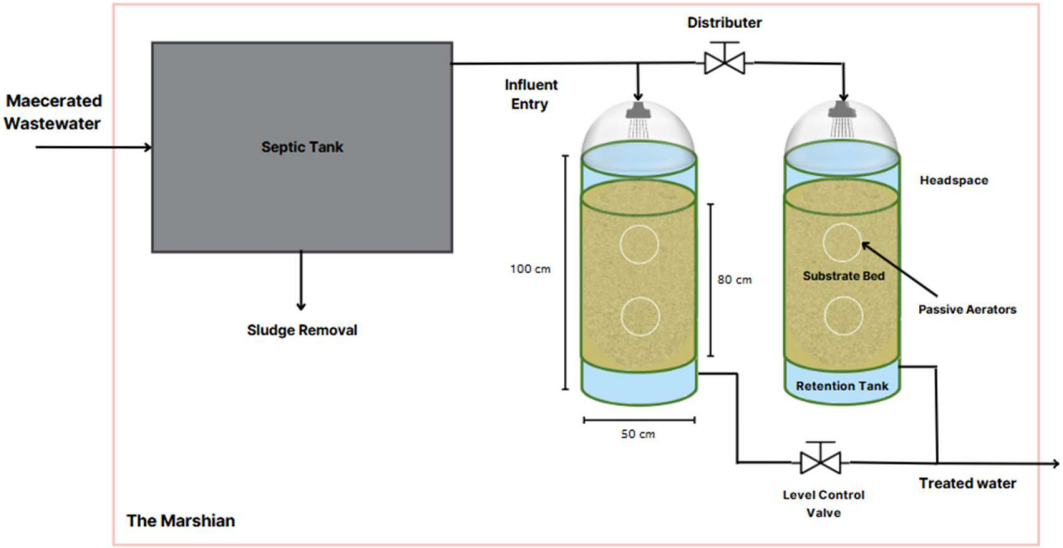

Figure 6.2.1: Figure shows the updated implementation to 'the Marshian' scenario based on recommendations on the simulation results

References

(1) Grove, P.; Fleischer, L. The Marshian: Conceptual Design of an Artificial Wetland for Waste Treatment on the Moon. **2024**.

(2) Fu, J.; Zhao, Y.; Yang, Y.; Yao, Q.; Ji, B.; Chen, S.; Dai, Y.; Tao, R.; Zhang, X. A Glance of Configuration-Operational Strategies and Intensification of Constructed Wetland towards Land-Effective Occupation. *J. Water Process Eng.* **2023**, *56*, 104473. https://doi.org/10.1016/j.jwpe.2023.104473.

(3) Nelson, M.; Finn, M.; Wilson, C.; Zabel, B.; van Thillo, M.; Hawes, P.; Fernandez, R. Bioregenerative Recycling of Wastewater in Biosphere 2 Using a Constructed Wetland: 2-Year Results. *Ecol. Eng.* **1999**, *13* (1), 189–197. https://doi.org/10.1016/S0925-8574(98)00099-8.

(4) Choudhary, A.; Kumar, S.; Sharma, C. Constructed Wetlands: An Approach for Wastewater Treatment; 2011.

(5) Selvamurugan, M.; Doraisamy, P.; Maheswari, M.; Nb, akumar. Constructed Wetlands for Wastewater Treatment: A Review. *Res. Rev. Biosci.* **2011**.

(6) Gröndahl, F.; Sidenmark, J.; Thomsen, A. Survey of Waste Water Disposal Practices at Antarctic Research Stations. *Polar Res.* **2009**, *28* (2), 298–306. https://doi.org/10.3402/polar.v28i2.6109.

(7) Voecks, G. E. In Situ Resource Utilization (ISRU). **2018**, 415–440. https://doi.org/10.1201/b22020-17.

(8) Advanced Propulsion Systems and Technologies, Today to 2020; Bruno, C., Accettura, A. G., Eds.; American Institute of Aeronautics and Astronautics: Reston ,VA, 2008. https://doi.org/10.2514/4.866937.

(9) Sacksteder, K.; Sanders, G. In-Situ Resource Utilization for Lunar and Mars Exploration. In *45th AIAA Aerospace Sciences Meeting and Exhibit*; Aerospace Sciences Meetings; American Institute of Aeronautics and Astronautics, 2007. https://doi.org/10.2514/6.2007-345.

(10) Epa, O. U. Wetlands Classification and Types; 2015.

(11) Zoltai, S. C. PEATLANDS AND MARSHES IN THE WETLAND REGIONS OF CANADA. *Mem. Entomol. Soc. Can.* **1987**, *119* (S140), 5–13. https://doi.org/10.4039/entm119140005-1.

(12) *Silica: an essential nutrient in wetland biogeochemistry - Struyf - 2009 - Frontiers in Ecology and the Environment - Wiley Online Library*. https://esajournals.onlinelibrary.wiley.com/doi/10.1890/070126 (accessed 2025-02-17).

(13) Guo, W. Overview on Wetlands Biogeochemistry; 2002.

(14) Jarvie, H. P.; Pallett, D. W.; Schäfer, S. M.; Macrae, M. L.; Bowes, M. J.; Farrand, P.; Warwick, A. C.; King, S. M.; Williams, R. J.; Armstrong, L.; Nicholls, D. J. E.; Lord, W. D.; Rylett, D.; Roberts, C.; Fisher, N. Biogeochemical and Climate Drivers of Wetland Phosphorus and Nitrogen Release: Implications for Nutrient Legacies and Eutrophication Risk. *J. Environ. Qual.* **2020**, *49* (6), 1703–1716. https://doi.org/10.1002/jeq2.20155.

(15) Qasaimeh, A.; AlSharie, H.; Masoud, T. A Review on Constructed Wetlands Components and Heavy Metal Removal from Wastewater. *J. Environ. Prot.* **2015**, *06* (07), 710–718. https://doi.org/10.4236/jep.2015.67064.

(16) Parde, D.; Patwa, A.; Shukla, A.; Vijay, R.; Killedar, D. J.; Kumar, R. A Review of Constructed Wetland on Type, Treatment and Technology of Wastewater. *Environ. Technol. Innov.* **2021**, *21*, 101261. https://doi.org/10.1016/j.eti.2020.101261.

(17) Vymazal, J. Constructed Wetlands for Wastewater Treatment: A Review; 2008.

(18) Zhang, D. Q.; Jinadasa, K. B. S. N.; Gersberg, R. M.; Liu, Y.; Ng, W. J.; Tan, S. K. Application of Constructed Wetlands for Wastewater Treatment in Developing Countries – A Review of Recent Developments (2000–2013). *J. Environ. Manage.* **2014**, *141*, 116–131. https://doi.org/10.1016/j.jenvman.2014.03.015.

(19) Swarnakar, A. K.; Bajpai, S.; Ahmad, I. Various Types of Constructed Wetland for Wastewater Treatment-A Review. *IOP Conf. Ser. Earth Environ. Sci.* **2022**, *1032* (1), 012026. https://doi.org/10.1088/1755-1315/1032/1/012026.

(20) Stefanakis, A. I. Constructed Wetlands: Description and Benefits of an Eco-Tech Water Treatment System. In *Waste Management*; Management Association, I. R., Ed.; IGI Global, 2020; pp 503–525. https://doi.org/10.4018/978-1-7998-1210-4.ch025.

(21) Cooper, P. The Performance of Vertical Flow Constructed Wetland Systems with Special Reference to the Significance of Oxygen Transfer and Hydraulic Loading Rates. *Water Sci. Technol. J. Int. Assoc. Water Pollut. Res.* **2005**, *51* (9), 81–90.

(22) Khanijo, I. Nutrient Removal from Wastewater by Wetland Systems; 2006.

(23) Meuleman, A. F. M.; Beekman, J. Ph.; Verhoeven, J. T. A. Nutrient Retention and Nutrient-Use Efficiency in Phragmites Australis Stands after Wasterwater Application. *Wetlands* **2002**, *22* (4), 712–721. https://doi.org/10.1672/0277-5212(2002)022[0712:NRANUE]2.0.CO;2.

(24) Shruthi, R.; Shivashankara, G. P. Investigation on the Performance Evaluation of Vertical Subsurface FLow Constructed Wetland for the Treatment of Rural Wastewater.

(25) I. Abdel-Shafy, H.; A. El-Khateeb, M. Integration of Septic Tank and Constructed Wetland for the Treatment of Wastewater in Egypt. *Desalination Water Treat.* **2013**, *51* (16–18), 3539–3546. https://doi.org/10.1080/19443994.2012.749585.

(26) Suresh, S.; Sharma, P.; Yaragal, R. R.; Mutnuri, S. Study on Effectiveness of Intervention of a Vertical Flow Constructed Wetland in between Septic Tank and Soak Pit for the Treatment of Septic Tank Effluent. *Nat. Environ. Pollut. Technol.* **2023**, *22* (1), 489–496. https://doi.org/10.46488/NEPT.2023.v22i01.047.

(27) Costa, V. A.; Queiroz, F. M. de; Oliveira, M. S.; Naves, P. L. F. Evaluation of Physicochemical and Microbiological Parameters of Wastewater Submitted to Constructed Wetland Treatment System. *Front. J. Soc. Technol. Environ. Sci.* **2022**, *11* (2), 131–140. https://doi.org/10.21664/2238-8869.2022v11i2.p131-140.

(28) Cui, Y.; Wang, W.; Chang, J. Study on the Product Characteristics of Pyrolysis Lignin with Calcium Salt Additives. *Materials* **2019**, *12* (10), 1609. https://doi.org/10.3390/ma12101609.

(29) Langergraber, G.; Haberl, R.; Laber, J.; Pressl, A. Evaluation of Substrate Clogging Processes in Vertical Flow Constructed Wetlands. *Water Sci. Technol.* **2003**, *48* (5), 25–34. https://doi.org/10.2166/wst.2003.0272.

(30) Samsó, R.; Garcia, J. BIO_PORE, a Mathematical Model to Simulate Biofilm Growth and Water Quality Improvement in Porous Media: Application and Calibration for Constructed Wetlands. *Ecol. Eng.* **2013**, *54*, 116–127. https://doi.org/10.1016/j.ecoleng.2013.01.021.

(31) Hoffmann, H.; Platzer, C.; von Münch, E.; Winker, M. Technology Review of Constructed Wetlands: Subsurface Flow Constructed Wetlands for Greywater and Domestic Wastewater Treatment; Deutsche Gesellschaft für Internationale Zusammenarbeit (GIZ) GmbH: Eschborn, Germany, 2011. (accessed 2023-09-10).

(32) Sklarz, M. Y.; Gross, A.; Yakirevich, A.; Soares, M. I. M. A Recirculating Vertical Flow Constructed Wetland for the Treatment of Domestic Wastewater. *Desalination* **2009**, *246* (1–3), 617–624. https://doi.org/10.1016/j.desal.2008.09.002.

(33) Phiijp, J. R. PHYSICS OF WATER MOVEMENT IN POROUS SOLIDS.

(34) *Nitrogen and Phosphorus Phytoextraction by Cattail (Typha spp.) during Wetland-based Phytoremediation of an End-of-Life Municipal Lagoon. | Semantic Scholar*. https://www.semanticscholar.org/paper/Nitrogen-and-Phosphorus-Phytoextraction-by-Cattail-Jeke-Zvomuya/2bb0e8603600fa1d7ba2cd0ef7da8d5cb3b5eb32 (accessed 2025-02-17).

(35) Hua, G.; Kong, J.; Ji, Y.; Li, M. Influence of Clogging and Resting Processes on Flow Patterns in Vertical Flow Constructed Wetlands. *Sci. Total Environ.* **2018**, *621*, 1142–1150. https://doi.org/10.1016/j.scitotenv.2017.10.113.

(36) Yang, C.; Zhang, X.; Tang, Y.; Jiang, Y.; Xie, S.; Zhang, Y.; Qin, Y. Selection and Optimization of the Substrate in Constructed Wetland: A Review. *J. Water Process Eng.* **2022**, *49*, 103140. https://doi.org/10.1016/j.jwpe.2022.103140.

(37) Sanford, W. E. Substrate Type, Flow Characteristics, and Detention Times Related to Landfill Leachate Treatment Efficiency in Constructed Wetlands. In *Constructed Wetlands for the Treatment of Landfill Leachates*; CRC Press, 1999.

(38) Gertsch, L.; Rostami, J.; Gustafson, R. Review of Lunar Regolith Properties for Design of Low Power Lunar Excavators; 2008.

(39) Carrier, W. D. GEOTECHNICAL PROPERTIES OF LUNAR SOIL.

(40) Alexander, D. B.; Zuberer, D. A.; Hubbell, D. H. Microbiological Considerations for Lunar-Derived Soils. In *ASA, CSSA, and SSSA Books*; Ming, D. W., Henninger, D. L., Eds.; American Society of Agronomy, Crop Science Society of America, Soil Science Society of America: Madison, WI, USA, 2015; pp 245–255. https://doi.org/10.2134/1989.lunarbaseagriculture.c18.

(41) Edmunson, J.; Betts, W.; Rickman, D.; Mclemore, C.; Fikes, J.; Stoeser, D.; Wilson, S.; Schrader, C. NASA Lunar Regolith Simulant Program; 2010.

(42) Sargeant, H.; Schultz, J.; Moser-Mancewicz, N.; Long-Fox, J.; Ustunisik, G.; Nielsen, R.; Britt, D. LUNAR SIMULANT CONSIDERATIONS FOR MOLTEN REGOLITH ELECTROLYSIS EXPERIMENTS; 2022.

(43) Sture, S. A Review of Geotechnical Properties of Lunar Regolith Simulants. In *Earth & Space 2006*; American Society of Civil Engineers: League City/Houston, Texas, United States, 2006; pp 1–6. https://doi.org/10.1061/40830(188)90.

(44) Or, D.; Tuller, M.; Jones, S. B. Liquid Behavior in Partially Saturated Porous Media under Variable Gravity. *Soil Sci. Soc. Am. J.* **2009**, *73* (2), 341–350. https://doi.org/10.2136/sssaj2008.0046.

(45) Sato, N.; Maruo, Y.; Naganuma, N.; Nogawa, K.; Aoki, S.; Noborio, K. Water Infiltration Rate in Fine Glass Beads under Micro- and Partial Gravities. *Adv. Space Res.* **2024**, *74* (8), 4189–4195. https://doi.org/10.1016/j.asr.2024.07.050.

(46) Schuerger, A. C.; Moores, J. E.; Smith, D. J.; Reitz, G. A Lunar Microbial Survival Model for Predicting the Forward Contamination of the Moon. *Astrobiology* **2019**, *19* (6), 730–756. https://doi.org/10.1089/ast.2018.1952.

(47) Allen, L. A.; Kalani, A. H.; Estante, F.; Rosengren, A. J.; Stodieck, L.; Klaus, D.; Zea, L. Simulated Micro-, Lunar, and Martian Gravities on Earth—Effects on Escherichia Coli Growth, Phenotype, and Sensitivity to Antibiotics. *Life* **2022**, *12* (9), 1399. https://doi.org/10.3390/life12091399.

(48) Kraner, H. W.; Schroeder, G. L.; Davidson, G.; Carpenter, J. W. Radioactivity of the Lunar Surface. *Science* **1966**, *152* (3726), 1235–1236. https://doi.org/10.1126/science.152.3726.1235.

(49) Darcy, H. (1803-1858) A. du texte. *Les Fontaines Publiques de La Ville de Dijon : Exposition et Application Des Principes à Suivre et Des Formules à Employer Dans Les Questions de Distribution d'eau... / Par Henry Darcy,...*; 1856.

(50) Soil Moisture. In *Climate Change and Terrestrial Ecosystem Modeling*; Bonan, G., Ed.; Cambridge University Press: Cambridge, 2019; pp 115–133. https://doi.org/10.1017/9781107339217.009.

(51) Chen, J.; Tong, H.; Yuan, J.; Fang, Y.; Gu, R. Permeability Prediction Model Modified on Kozeny-Carman for Building Foundation of Clay Soil. *Buildings* **2022**, *12* (11), 1798. https://doi.org/10.3390/buildings12111798.

(52) van Genuchten, M. Th. A Closed-Form Equation for Predicting the Hydraulic Conductivity of Unsaturated Soils. *Soil Sci. Soc. Am. J.* **1980**, *44* (5), 892–898. https://doi.org/10.2136/sssaj1980.03615995004400050002x.

(53) Yu, C.; Zheng, C. HYDRUS: Software for Flow and Transport Modeling in Variably Saturated Media. *Groundwater* **2010**, *48* (6), 787–791. https://doi.org/10.1111/j.1745-6584.2010.00751.x.

(54) Brozovich, C. DEMONSTRATION OF FLUID DYNAMICS FOR PLANT GROWING SYSTEMS IN VARIED GRAVITY ENVIRONMENTS THROUGH SCALED CAPILLARY MODELS.

(55) Sethi, R.; Di Molfetta, A. Mechanisms of Contaminant Transport in Aquifers. In *Groundwater Engineering : A Technical Approach to Hydrogeology, Contaminant Transport and Groundwater Remediation*; Sethi, R., Di Molfetta, A., Eds.; Springer International Publishing: Cham, 2019; pp 193–217. https://doi.org/10.1007/978-3-030-20516-4_10.

(56) Fetter, C. W.; Boving, T.; Kreamer, D. *Contaminant Hydrogeology*, Third edition.; Waveland Press, Inc: Long Grove, Illinois, 2018.

(57) Berkowitz, J. F.; Vepraskas, M. J.; Vaughan, K. L.; Vasilas, L. M. Development and Application of the Hydric Soil Technical Standard. *Soil Sci. Soc. Am. J.* **2021**, *85* (3), 469–487. https://doi.org/10.1002/saj2.20202.

(58) Shu, X.; Wu, Y.; Zhang, X.; Yu, F. Experiments and Models for Contaminant Transport in Unsaturated and Saturated Porous Media – A Review. *Chem. Eng. Res. Des.* **2023**, *192*, 606–621. https://doi.org/10.1016/j.cherd.2023.02.022.

(59) Langergraber, G. Modeling of Processes in Subsurface Flow Constructed Wetlands: A Review. *Vadose Zone J.* **2008**, *7* (2), 830–842. https://doi.org/10.2136/vzj2007.0054.

(60) Seigneur, N.; Mayer, K. U.; Steefel, C. I. Reactive Transport in Evolving Porous Media. *Rev. Mineral. Geochem.* **2019**, *85* (1), 197–238. https://doi.org/10.2138/rmg.2019.85.7.

(61) Mayer, K. U.; Frind, E. O.; Blowes, D. W. Multicomponent Reactive Transport Modeling in Variably Saturated Porous Media Using a Generalized Formulation for Kinetically Controlled Reactions. *Water Resour. Res.* **2002**, *38* (9), 13-1-13–21. https://doi.org/10.1029/2001WR000862.

(62) Šimůnek, J.; van Genuchten, M. Th.; Šejna, M. Recent Developments and Applications of the HYDRUS Computer Software Packages. *Vadose Zone J.* **2016**, *15* (7), vzj2016.04.0033. https://doi.org/10.2136/vzj2016.04.0033.

(63) Langergraber, G.; Šimůnek, J. Reactive Transport Modeling of Subsurface Flow Constructed Wetlands Using the HYDRUS Wetland Module. *Vadose Zone J.* **2012**, *11* (2), vzj2011.0104. https://doi.org/10.2136/vzj2011.0104.

(64) Langergraber, G.; Šimůnek, J. Modeling Variably Saturated Water Flow and Multicomponent Reactive Transport in Constructed Wetlands. *Vadose Zone J.* **2005**, *4* (4), 924–938. https://doi.org/10.2136/vzj2004.0166.

(65) Dittmer, U.; Meyer, D.; Langergraber, G. Simulation of a Subsurface Vertical Flow Constructed Wetland for CSO Treatment. *Water Sci. Technol. J. Int. Assoc. Water Pollut. Res.* **2005**, *51* (9), 225–232.

(66) *(PDF) Implementing Numerical Solvers for the Diffusion Equation*. ResearchGate. https://www.researchgate.net/publication/319998457_Implementing_Numerical_Solvers_for_the_Diffusion_Equation (accessed 2025-06-10).

(67) Jardin, S. C. The Galerkin Finite Element Method.

(68) Millington, R. J.; Quirk, J. P. Permeability of Porous Solids. *Trans. Faraday Soc.* **1961**, *57*, 1200. https://doi.org/10.1039/tf9615701200.

(69) Slyuta, E. N. Physical and Mechanical Properties of the Lunar Soil (a Review). *Sol. Syst. Res.* **2014**, *48* (5), 330–353. https://doi.org/10.1134/S0038094614050050.

(70) Ewert, M. K.; Chen, T. T.; Powell, C. D. Life Support Baseline Values and Assumptions Document. *Life Support*.

(71) Verostko, C. E.; Carrier, C.; Finger, B. W. *Ersatz Wastewater Formulations for Testing Water Recovery Systems*; SAE Technical Paper 2004-01–2448; SAE International: Warrendale, PA, 2004. https://doi.org/10.4271/2004-01-2448.

(72) Nasr, F. A.; Mikhaeil, B. Treatment of Domestic Wastewater Using Modified Septic Tank. *Desalination Water Treat.* **2015**, *56* (8), 2073–2081. https://doi.org/10.1080/19443994.2014.961174.

(73) Madier, D. The Fundamentals of Mesh Generation in Finite Element Analysis. **2023**.

(74) Langergraber, G.; Tietz, A.; Haberl, R. Comparison of Measured and Simulated Distribution of Microbial Biomass in Subsurface Vertical Flow Constructed Wetlands. *Water Sci. Technol.* **2007**, *56* (3), 233–240. https://doi.org/10.2166/wst.2007.496.

(75) Langergraber, G.; Šimůnek, J. Modeling Variably Saturated Water Flow and Multicomponent Reactive Transport in Constructed Wetlands. Hydrus CW2D Module Manual; Institute of Soil Biophysics, Czech Academy of Sciences: Prague, Czech Republic, 2005..

(76) Kadlec, R. H.; Wallace, S. D. Treatment Wetlands, 2nd ed.; CRC Press: Boca Raton, FL, 2008.

(77) Shrestha, B.; Hernandez, R.; Fortela, D. L. B.; Sharp, W.; Chistoserdov, A.; Gang, D.; Revellame, E.; Holmes, W. E.; Zappi, M. E. Formulation of a Simulated Wastewater Influent Composition for Use in the Research of Technologies for Managing Wastewaters Generated during Manned Long-Term Space

Exploration and Other Similar Situations—Literature-Based Composition Development. *BioTech* **2023**, *12* (1), 8. https://doi.org/10.3390/biotech12010008.

(78) Vera-Puerto, I.; Campal, J.; Martínez, S.; Cortés-Rico, L.; Coy, H.; Tan, S.; Arias, C. A.; Baquero-Rodríguez, G.; Rosso, D. Effects of Environmental Conditions and Bed Configuration on Oxygen Transfer Efficiency in Aerated Constructed Wetlands. *Water* **2022**, *14* (20), 3284. https://doi.org/10.3390/w14203284.

(79) Effect of Low Dissolved Oxygen on Simultaneous Nitrification and Denitrification in a Membrane Bioreactor Treating Black Water. *Bioresour. Technol.* **2011**, *102* (6), 4333–4340. https://doi.org/10.1016/j.biortech.2010.11.096.

(80) Council of the European Communities. Council Directive of 21 May 1991 concerning urban waste water treatment (91/271/EEC). Off. J. Eur. Communities 1991, L135, 40–52..

(81) Tabuchi, Y.; Kioka, A.; Yamada, Y. Water Permeability of Sunlit Lunar Highlands Regolith Using LHS-1 Simulant. *Acta Astronaut.* **2023**, *213*, 344–354. https://doi.org/10.1016/j.actaastro.2023.09.027.

(82) Chevrier, V.; Sears, D. W. G.; Chittenden, J. D.; Roe, L. A.; Ulrich, R.; Bryson, K.; Billingsley, L.; Hanley, J. Sublimation Rate of Ice under Simulated Mars Conditions and the Effect of Layers of Mock Regolith JSC Mars-1. *Geophys. Res. Lett.* **2007**, *34* (2). https://doi.org/10.1029/2006GL028401.

(83) Long-Fox, J.; Perman, J.; Z; Landsman; Metke, A.; Britt, D. Investigating the Effects of Composition on Granular Surface Area: Gas Sorption Analyses of High-Fidelity Lunar Highlands and Carbonaceous Chondrite Asteroid Regolith Simulants; 2022.

(84) Jones, S. B.; Or, D.; Heinse, R.; Tuller, M. Beyond Earth: Designing Root Zone Environments for Reduced Gravity Conditions. *Vadose Zone J.* **2012**, *11* (1), vzj2011.0081. https://doi.org/10.2136/vzj2011.0081.

(85) Wang, K.; Huang, G. Impact of Hydraulic Conductivity on Solute Transport in Highly Heterogeneous Aquifer. In *Computer and Computing Technologies in Agriculture IV*; Li, D., Liu, Y., Chen, Y., Eds.; IFIP Advances in Information and Communication Technology; Springer Berlin Heidelberg: Berlin, Heidelberg, 2011; Vol. 344, pp 643–655. https://doi.org/10.1007/978-3-642-18333-1_78.

(86) *Fate and Transport of Subsurface Pollutants*; Gupta, P. K., Bharagava, R. N., Eds.; Microorganisms for Sustainability; Springer Singapore: Singapore, 2021; Vol. 24. https://doi.org/10.1007/978-981-15-6564-9.

(87) Fondjo, S. A. A.; Theron, E.; Ray, R. Assessment of Various Methods to Measure the Soil Suction. *Int. J. Innov. Technol. Explor. Eng.* **2020**, *9*, 171–184. https://doi.org/10.35940/ijitee.L7958.1091220.

(88) Maruo, Y.; Sato, N.; Nogawa, K.; Aoki, S.; Noborio, K. Pore-Scale Wetting Process of Capillary-Driven Flow in Unsaturated Porous Media under Micro- and Earth-Gravities. *Water* **2022**, *14* (13), 1995. https://doi.org/10.3390/w14131995.

(89) Wanko, A.; Forquet, N.; Mose, R.; Sadowski, A.-G. Using Fluorescence for a Full Spectral Analysis of Dissolved and Gaseous Oxygen within a Sand Bed. In *Water Pollution VIII: Modelling, Monitoring and Management*; WIT Press: Bologna, Italy, 2006; Vol. 1, pp 369–378. https://doi.org/10.2495/WP060371.

(90) Lucke, T.; Walker, C.; Beecham, S. Experimental Designs of Field-Based Constructed Floating Wetland Studies: A Review. *Sci. Total Environ.* **2019**, *660*, 199–208. https://doi.org/10.1016/j.scitotenv.2019.01.018.

(91) Liu, H.; Hu, Z.; Zhang, J.; Ngo, H. H.; Guo, W.; Liang, S.; Fan, J.; Lu, S.; Wu, H. Optimizations on Supply and Distribution of Dissolved Oxygen in Constructed Wetlands: A Review. *Bioresour. Technol.* **2016**, *214*, 797–805. https://doi.org/10.1016/j.biortech.2016.05.003.

(92) Arias, L.; Bertrand-Krajewski, J.-L.; Molle, P. Simplified Hydraulic Model of French Vertical-Flow Constructed Wetlands. *Water Sci. Technol.* **2014**, *70* (5), 909. https://doi.org/10.2166/wst.2014.309.

(93) Letey, J.; Jarrell, W. M.; Valoras, N. Nitrogen and Water Uptake Patterns and Growth of Plants at Various Minimum Solution Nitrate Concentrations. *J. Plant Nutr.* **1982**, *5* (2), 73–89. https://doi.org/10.1080/01904168209362939.

(94) Heiken, G. H.; Vaniman, D. T.; French, B. M. *Lunar Sourcebook - A User's Guide to the Moon*; ISBN: 0-521-33444-6; 1991. https://ntrs.nasa.gov/citations/19920057201 (accessed 2025-03-03).

(95) Giraldi, D.; De Michieli Vitturi, M.; Iannelli, R. FITOVERT: A Dynamic Numerical Model of Subsurface Vertical Flow Constructed Wetlands. *Environ. Model. Softw.* **2010**, *25* (5), 633–640. https://doi.org/10.1016/j.envsoft.2009.05.007.

(96) Petitjean, A.; Wanko, A.; Forquet, N.; Mosé, R.; Lawniczak, F.; Sadowski, A. Diphasic Transfer of Oxygen in Vertical Flow Filters: A Modelling Approach. *Water Sci. Technol.* **2011**, *64* (1), 109–116. https://doi.org/10.2166/wst.2011.618.

(97) Schreiner, S. S.; Dominguez, J. A.; Sibille, L.; Hoffman, J. A. Thermophysical Property Models for Lunar Regolith. Adv. Space Res. 2016, 57 (5), 1209–1222

(98) Tian, X.; Zhao, C.; Ji, X.; Feng, T.; Liu, Y.; Bian, D. The Correlation Analysis of TOC and $COD_{(Cr)}$ in Urban Sewage Treatment. E3S Web Conf. 2019, 136, 06010. DOI: 10.1051/e3sconf/201913606010

Annex

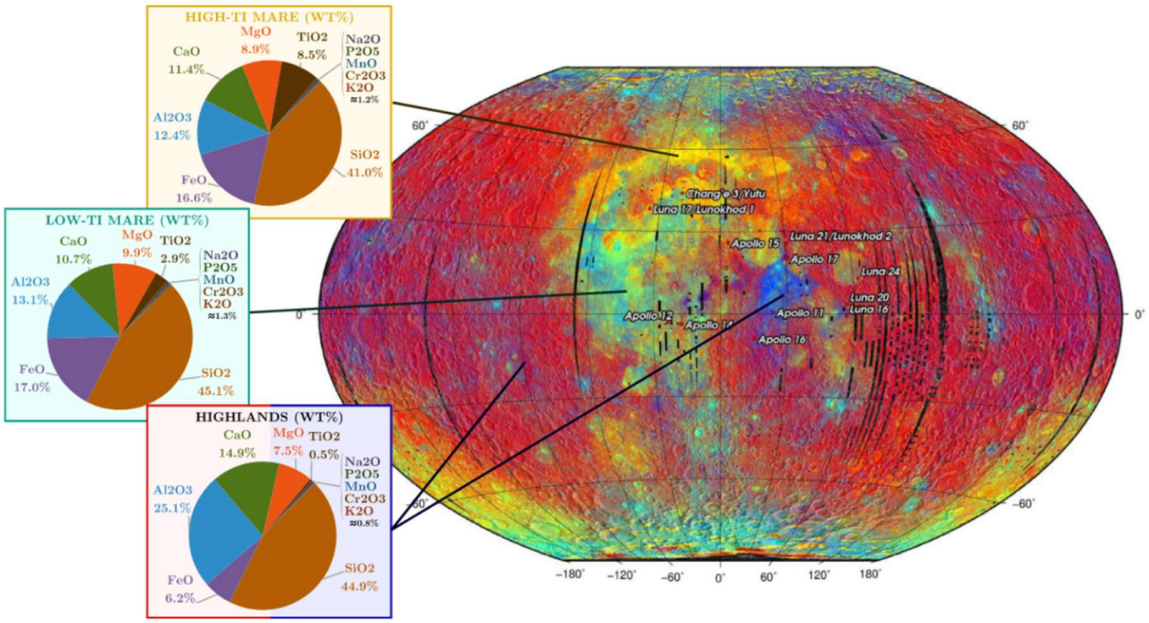

Figure A1: Figure shows the mineral composition of different lunar regoliths depending upon their geolocation on the moon as shown in Schreiner et al., 2016[97]

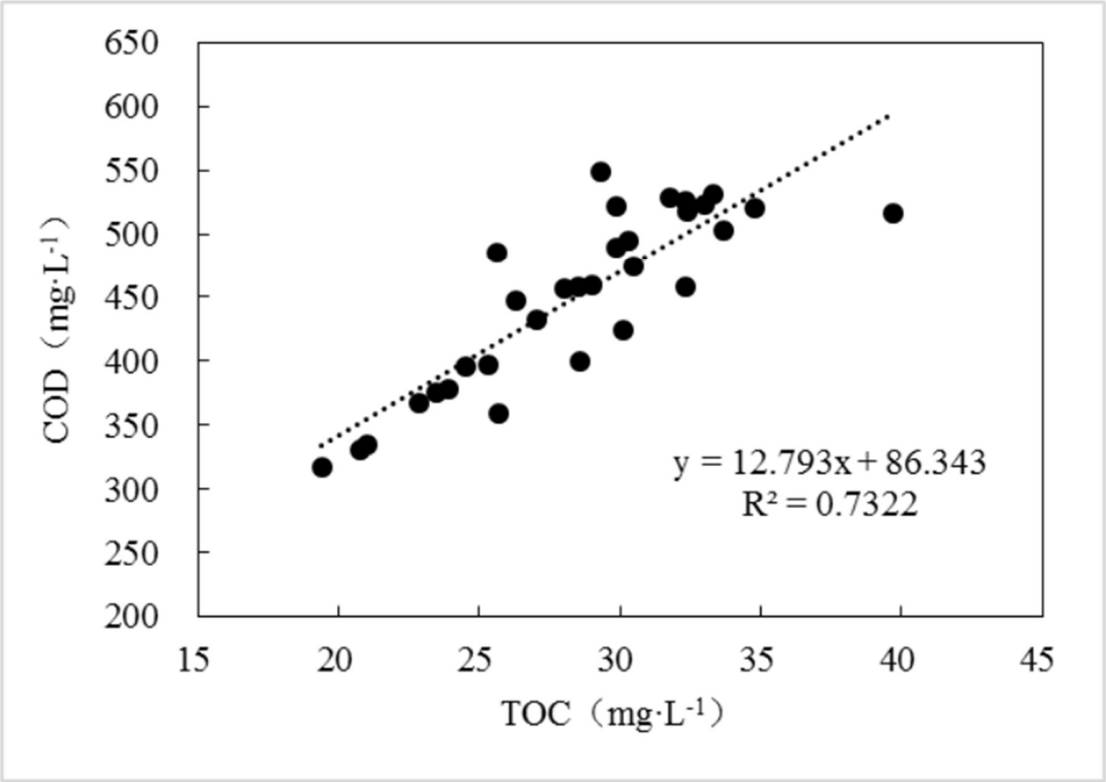

Figure A2: Figure shows the correlation between total organic carbon (TOC) and carbon oxygen demand (COD) for urban wastewater as shown in Tian et al., 2019[98]

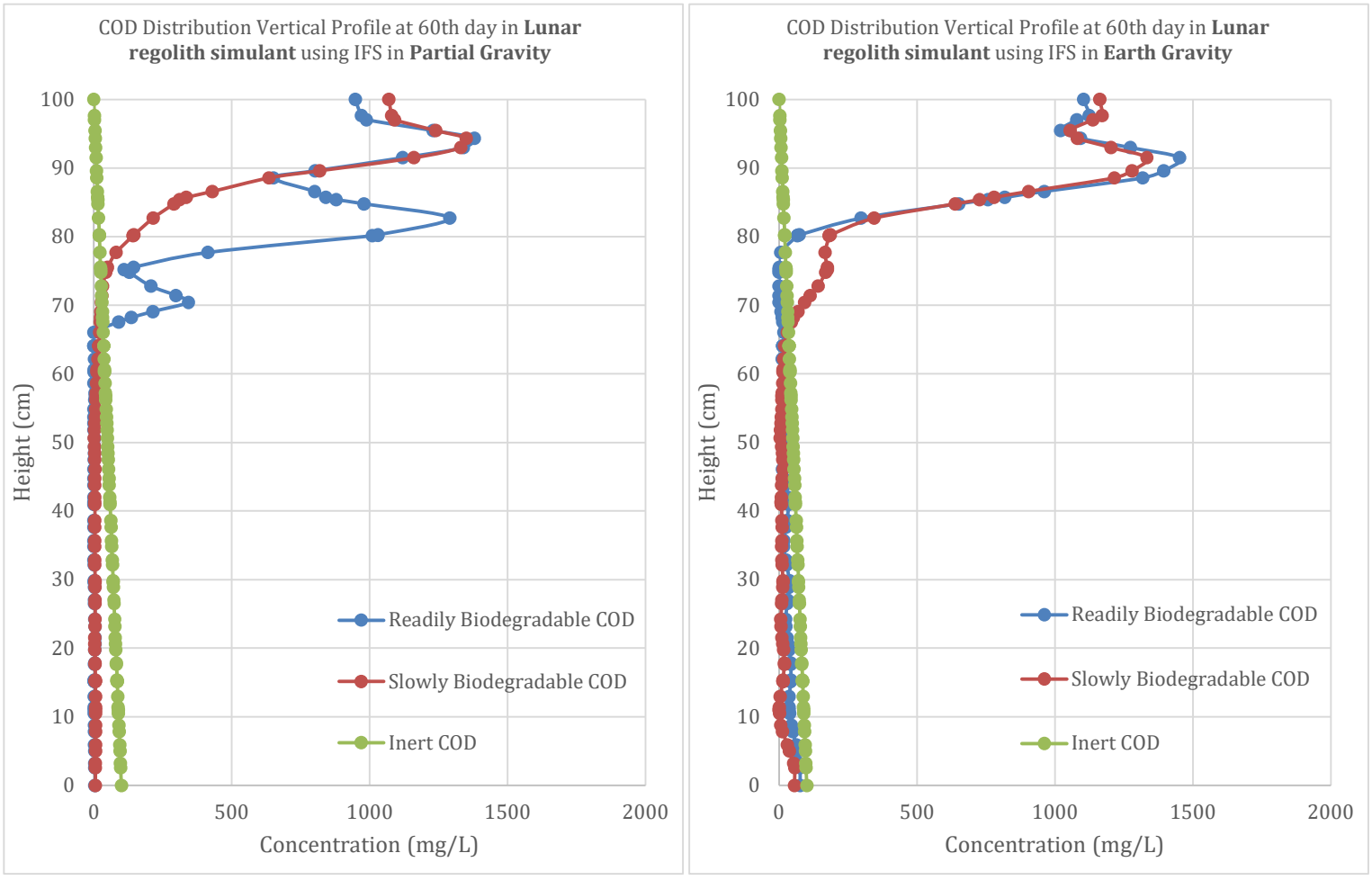

Figure A3: Figure shows the COD distribution over the height of the lunar regolith simulant bed at 60th day using IFS in partial (left) and earth (right) gravity conditions

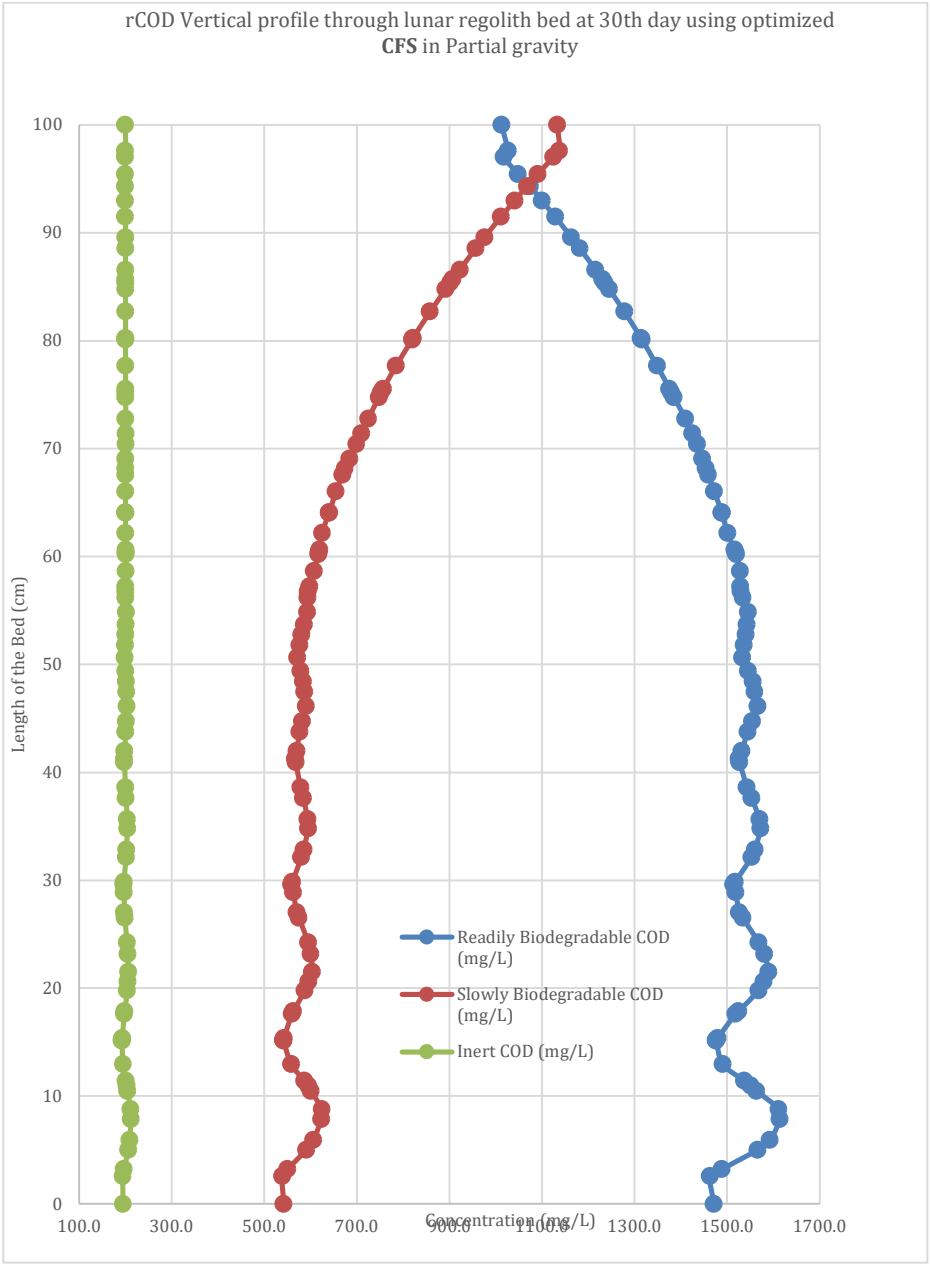

Figure A4: Figure shows the COD distribution over the height of the lunar regolith simulant bed at 30th day using optimized CFS in partial gravity conditions

Tables

Table A1: Table shows the speculations of particle size distribution of lunar regolith as pointed out in Heiken et al., 1991[94]

Depth Range (cm)	Average Porosity, n (%)	Average Void Ratio, e
0 – 15	52 ± 2	1.07 ± 0.07
0 – 30	49 ± 2	0.96 ± 0.07
30 – 60	44 ± 2	0.78 ± 0.07
0 – 60	46 ± 2	0.87 ± 0.07

Table A2. Table shows the summary of software review for modeling of VFCW in partial gravity using different substrates

Model	Application	Availability	Pros, Cons & Source
HYDRUS-2D CW2D/CWM1	HFCWs and VFCWs for domestic and other wastewaters	Commercial (HYDRUS software)	Pros: Graphical user interface, detailed multi-component reactive transport, includes DO, OM, and nitrogen pathways, handles variably saturated flow.
			Cons: Expensive, clogging not considered, limited gravity settings, only models dissolved substances.
			Source: Langergraber & Šimůnek, 2005[64]
FITOVERT (MATLAB)	VFCWs under unsaturated conditions, with evapotranspiration	Not publicly available	Pros: Models non-typical feeding/emptying cycles, simulates clogging via porosity reduction, includes particulate transport.
			Cons: No plant uptake or adsorption modeling, phosphorus and persistent pollutants not simulated.
			Source: Giraldi et al., 2009[95]
Diph_M (MATLAB)	2nd stage French VFCWs, post-septic tank treatment	Not accessible	Pros: Diphasic air-water modeling, tracks DO, ammonium, and COD transport.
			Cons: Based on older CW1 model, limited accessibility for use or testing.
			Source: Petitjean et al., 2012[96]
RSF_Sim	CWs for combined sewer overflow (CSO) treatment	Open access for scientific use	Pros: Designed for dynamic Combined Sewer Overloads, suitable for integration with sewer system models.
			Cons: Not applicable for domestic wastewater or nutrient-focused systems.
			Source: Meyer & Dittmer, 2015[65]

Table A3: The table shows physical and mechanical properties of lunar regolith (Slyuta et al., 2013)[69] used for estimation of solute transport properties of lunar regolith simulant

Characteristics		Numerical value
Soil density	Surface layer	1.3 g/cm^3
	At the depth of 15.0 cm	1.5 g/cm^3
	At the depth of 60 cm	1.66 g/cm^3
	At the depth of 200 cm	1.9 g/cm^3
Density variation	To the depth of 200 cm	$\rho = 1.92(z + 12.2)/(z + 18)$
Soil porosity	Surface layer 0–15 cm	52 ± 2%
	At the depth of 30–60 cm	44 ± 2%
Porosity variation	To the depth of 200 cm	≤40%
Percentage (%) of grains larger than the assumed value for the typical lunar regolith $N_{>d}\% = -23.205\ln(d) + 143.586$	>841 μm	1%
	>250 μm	15%
	>105 μm	35%
	>53 μm	50%
	>20 μm	78%
Soil deformation modulus	Surface layer	15.6–29 kPa
	At the depth of 200 cm	240 kPa
Deformation modulus variation	To the depth of 200 cm	15.6–240 kPa
Poisson ratio of the soil (mean value)	To the depth of 200 cm	0.2
Shear strength of the soil	At the depth of 5 cm	0.1–2.5 kPa
	At the depth of 50 cm	1–3.5 kPa
	At the depth of 100 cm	2–4 kPa
	At the depth of 200 cm	4–8 kPa
Shear strength variation	To the depth of 200 cm	0.1–8 kPa
Cohesion of grains (mean value)	At the depth of 0–15 cm	0.52 kPa
	At the depth of 10–20 cm	0.6 kPa
	At the depth of 0–30 cm	0.90 kPa
	At the depth of 30–60 cm	3.0 kPa
	At the depth of 0–60 cm	1.6 kPa
Cohesion variation	To the depth of 200 cm	0.1–3.5 kPa
Variation of the internal friction angle	To the depth of 200 cm	30°–50°

Table A4: The table shows the distribution of wastewater in an early planetary base as a baseline assumption value for typical steady-state wastewater generation rates for various missions (Ewert et al., 2022)[70]

Parameter	Units	International Space Station	Transit Vehicle	Early Planetary Base	Mature Planetary Base
Urine	kg/CM-d	1.20 (1)	1.50 (2)	1.50 (2)	1.50 (2)
Urinal Flush	kg/CM-d	0.30 (1)	0.30 (1)	0.50 (2)	0.50 (2)
Total Urine Wastewater Load	*kg/CM-d*	*1.50*	*1.80*	*2.00*	*2.00*
Oral Hygiene	kg/CM-d	n/a	n/a	0.37 (2)	0.37 (2)
Hand Wash	kg/CM-d	n/a	n/a	4.08 (2)	4.08 (2)
Shower [92]	kg/CM-d	n/a	n/a	1.08 (5)	1.08 (5)
Laundry	kg/CM-d	n/a	n/a	n/a	1.1 (6)
Dish Wash	kg/CM-d	n/a	n/a	n/a	3.54 (5)
Food Preparation and Processing	kg/CM-d	n/a	n/a	n/a	TBD
Total Hygiene Wastewater Load	*kg/CM-d*	*0.00*	*0.00*	*5.53*	*10.17+*
Crew Latent Humidity Condensate	kg/CM-d	2.27 (2)	2.27 (2)	2.27 (2)	2.90 (2)
Animal Latent Humidity Condensate	kg/CM-d	n/a	n/a	TBD	TBD
Total Latent Wastewater Load	*kg/CM-d*	*2.27*	*2.27*	*2.27+*	*2.90+*
Payload	kg/CM-d	n/a	n/a	TBD (3)	TBD (3)
Total Payload Wastewater Load	*kg/CM-d*	*0.00*	*0.00*	*0.00+*	*0.00+*
Total Wastewater Load	***kg/CM-d***	***3.77***	***4.07***	***9.80+***	***15.07+***
Biomass Production Wastewater [93]	$kg/m^2 \cdot d$	n/a	n/a	n/a	TBD

Table A5: The table shows the measured parameters for ERSATZ formulation of wastewater from an early planetary base[71]

Ersatz		pH	Conductivity (µS)	TOC (mg/l)	TIC (mg/l)	Chloride (mg/l)	Nitrite-N (mg/l)	Nitrate-N (mg/l)
Transit Wastewater	Analog Target	- [3]	-	2199	33 [4]	1887	-	-
	Ersatz Formulation [1]	2.6 ± 0.2	12352 ± 1853	2209 ± 221	0 ± 0	1870 ± 281	-	-
	Measurement Results [2]	2.72 ± 0.01	12352 ± 53	2233 ± 34	0 ± 0	1852 ± 6.5	-	-
Early Planetary Base Wastewater	IWRS Test Data	8.9 ± 0.2	6400 ± 1300	519 ± 118	325 -	515 ± 204	-	-
	Ersatz Formulation	8.9 ± 0.2	6869 ± 1030	631 ± 63	391 ± 59	514 ± 77	-	-
	Measurement Results	8.83 ± 0.01	6869 ± 23	631 ± 16	399 ± 12	525 ± 8.8	-	-
BWP Effluent	IWRS Test Data	6.5 ± 0.4	3281 ± 710	48 ± 23	72 ± 63	515 ± 204	3.0 ± 2.8	27 ± 19
	Ersatz Formulation	6.6 ± 0.2	3802 ± 570	51 ± 5.1	110 ± 17	608 ± 91	5.0 ± 0.7	47 ± 7.1
	Measurement Results	6.76 ± 0.01	3802 ± 48	58 ± 0.8	97 ± 4	723 ± 28	5.4 ± 0.1	46 ± 1.1
RO Permeate - Nominal	IWRS Test Data	6.3 ± 0.4	330 ± 157	1.2 ± 1.2	14 ± 6	26 ± 15	1.8 ± 1.8	8.4 ± 7.5
	Ersatz Formulation	6.6 ± 0.2	285 ± 43	1.4 ± 0.5	14.0 ± 2.1	32.0 ± 4.8	1.8 ± 0.3	5.1 ± 0.8
	Measurement Results	6.67 ± 0.01	285 ± 3.2	1.3 ± 0.2	13.9 ± 0.1	30.85 ± 0.3	1.57 ± 0.01	4.9 ± 0.1
RO Permeate - Worst Case	IWRS Test Data [5]	-	487	5.3	20	41	1.8	1.81
	Ersatz Formulation	7.3 ± 0.2	382 ± 57	5.0 ± 1.5	17.9 ± 2.7	62.0 ± 9.3	2.8 ± 0.4	6.6 ± 1.0
	Measurement Results	7.45 ± 0.04	382 ± 2.4	5.2 ± 0.4	18.2 ± 0.2	56.5 ± 0.5	2.68 ± 0.02	6.3 ± 0.1
AES Condensate - Nominal	IWRS Test Data	8.0 ± 0.6	471 ± 403	3.9 ± 2.6	37 ± 24	-	-	-
	Ersatz Formulation	8.0 ± 0.2	507 ± 76	4.5 ± 1.5	52 ± 7.8	-	-	-
	Measurement Results	8.00 ± 0.01	507 ± 1.7	5.8 ± 0.1	54.1 ± 0.6	-	-	-
AES Condensate - Worstcase	IWRS Test Data	9.4 ± 0.1	1917 ± 971	6.3 ± 5.0	93 ± 14	-	-	-
	Ersatz Formulation	9.4 ± 0.2	1286 ± 193	9.5 ± 3.0	94.0 ± 14.1	-	-	-
	Measurement Results	9.54 ± 0.01	1286 ± 235	12.4 ± 0.1	114 ± 0.7	-	-	-

Table A6: Table shows the kinetic parameters used for reactive transport simulations for microbial conversions, taken from HYDRUS-manual[75]

Kinetic parameter		Value	
		20°C	10°C
K_h	hydrolysis rate constant [1/d]	3	2
K_X**	sat./inh. coeff. for hydrolysis [$mg_{COD,CS}/mg_{COD,BM}$]	0.1	0.22
μ_H	maximum aerobic growth rate on CR [1/d]	6	3
b_H	rate constant for lysis [1/d]	0.4	0.2
$K_{het,O2}$	sat./inh. coeff. for O2 [mg_{O2}/l]	0.2	0.2
$K_{het,CR}$	sat./inh. coeff. for substrate [$mg_{COD,CR}/l$]	2	2
$K_{het,NH4N}$	sat./inh. coeff. for NH4 (nutrient) [mg_{NH4N}/l]	0.05	0.05
$K_{het,IP}$	sat./inh. coeff. for P [mg_{IP}/l]	0.01	0.01
μ_{DN}	maximum denitrification rate [1/d]	4.8	2.4
$K_{DN,O2}$	sat./inh. coeff. for O2 [mg_{O2}/l]	0.2	0.2
$K_{DN,NO3N}$	sat./inh. coeff. for NO3 [mg_{NO3N}/l]	0.5	0.5
$K_{DN,NO2N}$	sat./inh. coeff. for NO2 [mg_{NO2N}/l]	0.5	0.5
$K_{DN,CR}$	sat./inh. coeff. for substrate [$mg_{COD,CR}/l$]	4	4
$K_{DN,NH4N}$	sat./inh. coeff. for NH4 (nutrient) [mg_{NH4N}/l]	0.05	0.05
$K_{DN,IP}$	sat./inh. coeff. for P [mg_{IP}/l]	0.01	0.01
μ_{ANs}*	maximum aerobic growth rate on NH4N [1/d]	0.9	0.3
b_{ANs}*	rate constant for lysis [1/d]	0.15	0.05
$K_{ANs,O2}$*	sat./inh. coeff. for O2 [mg_{O2}/l]	1	1
$K_{ANs,NH4N}$**	sat./inh. coeff. for NH4 [mg_{NH4N}/l]	0.5	5.0
$K_{ANs,IP}$	sat./inh. coeff. for P [mg_{IP}/l]	0.01	0.01
μ_{ANb}*	maximum aerobic growth rate on NO2N [1/d]	1	0.35
b_{ANb}*	rate constant for lysis [1/d]	0.15	0.05
$K_{ANb,O2}$*	sat./inh. coeff. for O2 [mg_{O2}/l]	0.1	0.1
$K_{ANb,NO2N}$*	sat./inh. coeff. for NO2 [mg_{NO2N}/l]	0.1	0.1
$K_{ANb,NH4N}$	sat./inh. coeff. for NH4 (nutrient) [mg_{NH4N}/l]	0.05	0.05
$K_{ANb,IP}$	sat./inh. coeff. for P [mg_{IP}/l]	0.01	0.01

* Nowak (1996), ** Langergraber (2005b).

Table A7: Table shows the molecular diffusion coefficients used for different contaminant components taken from HYDRUS wetland example 1[75]

Solute	Molecular Dispersion Coefficient in Free Water (cm^2/day)	Molecular Dispersion Coefficient in Soil Air (cm^2/day)
Dissolved Oxygen	0.00072	769
Readily biodegradable rCOD	0.000456	0
Slowly biodegradable sCOD	0.000456	0
Inert chemical oxygen demand iCOD	0.000456	0
Heterotrophic microorganism	0	0
Nitrosomonas spp. (autotrophic bacteria 1)	0	0
Nitrobacter spp. (autotrophic bacteria 2)	0	0
Ammonium ion (NH4+)	0.000801	0
Nitrite ion (NO_2^-)	0.000801	0
Nitrate ion (NO_3^-)	0.000801	0
Dinitrogen gas (N_2)	0.000801	0
Phosphorus (inorganic)	0.000801	0

Table A8: Table shows the reactions modelled in HYDRUS-2D using CW2D module and their rate expressions[75]

R	Process / Reaction rate rc_j	
Heterotrophic organisms		
1	Hydrolysis	
	$rc_1 = K_h \cdot \frac{c_{CS}/c_{XH}}{K_X + c_{CS}/c_{XH}} \cdot c_{XH}$	(3.2)
2	Aerobic growth of heterotrophs on readily biodegradable COD	
	$rc_2 = \mu_H \cdot \frac{c_{O2}}{K_{Het,O2} + c_{O2}} \cdot \frac{c_{CR}}{K_{Het,CR} + c_{CR}} \cdot f_{N,Het} \cdot c_{XH}$	(3.3)
3	NO3-growth of heterotrophs on readily biodegradable COD	
	$rc_3 = \mu_{DN} \cdot \frac{K_{DN,O2}}{K_{DN,O2} + c_{O2}} \cdot \frac{c_{NO3}}{K_{DN,NO3} + c_{NO3}} \cdot \frac{K_{DN,NO2}}{K_{DN,NO2} + c_{NO2}} \cdot \frac{c_{CR}}{K_{DN,CR} + c_{CR}} \cdot f_{N,DN} \cdot c_{XH}$	(3.4)
4	NO2-growth of heterotrophs on readily biodegradable COD	
	$rc_4 = \mu_{DN} \cdot \frac{K_{DN,O2}}{K_{DN,O2} + c_{O2}} \cdot \frac{c_{NO2}}{K_{DN,NO2} + c_{NO2}} \cdot \frac{c_{CR}}{K_{DN,CR} + c_{CR}} \cdot f_{N,DN} \cdot c_{XH}$	(3.5)
5	Lysis of heterotrophs	
	$rc_5 = b_H \cdot c_{XH}$	(3.6)
Autotrophic organisms 1 – *Nitrosomonas*		
6	Aerobic growth of *Nitrosomonas* on NH4	
	$rc_6 = \mu_{ANs} \cdot \frac{c_{O2}}{K_{ANs,O2} + c_{O2}} \cdot \frac{c_{NH4}}{K_{ANs,NH4} + c_{NH4}} \cdot \frac{c_{IP}}{K_{ANs,IP} + c_{IP}} \cdot c_{XANs}$	(3.7)
7	Lysis of *Nitrosomonas*	
	$rc_7 = b_{HANs} \cdot c_{XANs}$	(3.8)
Autotrophic organisms 2 – *Nitrobacter*		
8	Aerobic growth of *Nitrobacter* on NO2	
	$rc_8 = \mu_{ANb} \cdot \frac{c_{O2}}{K_{ANb,O2} + c_{O2}} \cdot \frac{c_{NO2}}{K_{ANb,NO2} + c_{NO2}} \cdot f_{N,ANb} \cdot c_{XANb}$	(3.9)
9	Lysis of *Nitrobacter*	
	$rc_9 = b_{HANb} \cdot c_{XANb}$	(3.10)
Conversion of solid in liquid phase concentrations		
	$c_{XY} = \frac{\rho}{\theta} \cdot s_{XY}$, where $Y = H, ANs, ANb$	(3.11)
Factor for nutrients		
	$f_{N,x} = \frac{c_{NH4}}{K_{x,NH4} + c_{NH4}} \cdot \frac{c_{IP}}{K_{x,IP} + c_{IP}}$, where $x = Het, DN, ANb$	(3.12)

The stoichiometric coefficients of these parameters can be found in HYDRUS CW2D module.[75]

Supporting Information

S1. Reactions modelled in CW2D Module[75]

Heterotrophic Bacteria Processes

These bacteria are responsible for breaking down organic matter and performing both aerobic and anoxic processes as explained in HYDRUS CW2D manual:[75]

Hydrolysis: Slowly biodegradable compounds are broken down into simpler, more readily degradable forms (rCOD). This reaction also releases ammonium (NH_4^+) and orthophosphate (IP). Hydrolysis occurs regardless of oxygen presence.

Aerobic Growth: Under oxygen-rich conditions, heterotrophs consume readily biodegradable COD (rCOD) and oxygen (O_2) while incorporating NH_4^+ and IP into new biomass.

Anoxic Growth (Denitrification): In oxygen-limited conditions, heterotrophs use nitrate (NO_3^-) or nitrite (NO_2^-) as electron acceptors, converting them into dinitrogen gas (N_2). This process also consumes CR, NH_4^+, and IP.

Lysis: When heterotrophs die, they release organic matter (COD), along with NH_4^+ and IP, back into the system.

Autotrophic Bacteria Processes

These microorganisms are specialized for nitrification, which occurs in two aerobic steps:

Step 1 – Nitrosomonas Activity: These bacteria oxidize NH_4^+ into NO_2^-, consuming O_2 in the process. Some NH_4^+ and IP are assimilated into the biomass.

Step 2 – Nitrobacter Activity: In the next step, NO_2^- is further oxidized to NO_3^-, with continued uptake of O_2, NH_4^+, and IP into biomass.

Autotroph Lysis: Similar to heterotrophs, the breakdown of autotrophic biomass releases organic matter, NH_4^+, and IP into the system.